Thin film flow down a porous substrate in the presence of an insoluble surfactant : Stability analysis

A. Anjalaiah, R. Usha, S éverine Millet

PHYSICS OF FLUIDS **25**, 022101 (2013)

Thin film flow down a porous substrate in the presence of an insoluble surfactant: Stability analysis

Anjalaiah,[1,a] R. Usha,[1,b] and S. Millet[2,c]
[1]*Department of Mathematics, Indian Institute of Technology Madras, Chennai 600 036, India*
[2]*Université de Lyon, Université Lyon 1, INSA-Lyon, École centrale de Lyon, Laboratorire de Méchanique des Fluides et d'Acoustique UMR CNRS 5509, F-69621, Lyon, France*

(Received 18 May 2012; accepted 5 January 2013; published online 1 February 2013)

The stability of a gravity-driven film flow on a porous inclined substrate is considered, when the film is contaminated by an insoluble surfactant, in the frame work of Orr-Sommerfeld analysis. The classical long-wave asymptotic expansion for small wave numbers reveals the occurrence of two modes, the Yih mode and the Marangoni mode for a clean/a contaminated film over a porous substrate and this is confirmed by the numerical solution of the Orr-Sommerfeld system using the spectral-Tau collocation method. The results show that the Marangoni mode is always stable and dominates the Yih mode for small Reynolds numbers; as the Reynolds number increases, the growth rate of the Yih mode increases, until, an exchange of stability occurs, and after that the Yih mode dominates. The role of the surfactant is to increase the critical Reynolds number, indicating its stabilizing effect. The growth rate increases with an increase in permeability, in the region where the Yih mode dominates the Marangoni mode. Also, the growth rate is more for a film (both clean and contaminated) over a thicker porous layer than over a thinner one. From the neutral stability maps, it is observed that the critical Reynolds number decreases with an increase in permeability in the case of a thicker porous layer, both for a clean and a contaminated film over it. Further, the range of unstable wave number increases with an increase in the thickness of the porous layer. The film flow system is more unstable for a film over a thicker porous layer than over a thinner one. However, for small wave numbers, it is possible to find the range of values of the parameters characterizing the porous medium for which the film flow can be stabilized for both a clean film/a contaminated film as compared to such a film over an impermeable substrate; further, it is possible to enhance the instability of such a film flow system outside of this stability window, for appropriate choices of the porous substrate characteristics. © *2013 American Institute of Physics*. [http://dx.doi.org/10.1063/1.4789459]

I. INTRODUCTION

The flow of a thin liquid film down an inclined plane or a vertical wall in the presence of a free surface displays a variety of spatio-temporal patterns. The wave structures that occur on the surface of such films have attracted the attention of several investigators and there has been a significant amount of theoretical, computational, and experimental studies on the dynamics and stability of such flow systems under the influence of several factors that have technological and industrial applications.[1–4] The occurrence of such waves is a desirable feature in cooling of films. On the other hand, in coating flows, the presence of surface waves is not desired, since a smooth surface is usually desired as a finished product. In view of different applications of such flows, one should look for

[a]E-mail: anjimaths20@gmail.com.
[b]Author to whom correspondence should be addressed. Electronic mail: ushar@iitm.ac.in.
[c]E-mail: severine.millet@univ-lyon1.fr.

strategies to control or suppress the free surface instabilities. It has been shown that, one can suppress the free-surface instabilities by choosing appropriately the amplitudes and the frequencies of the forced oscillations of the bottom wall[5] and outside these windows of stability, one can enhance the instability of the film. Demekhin *et al.*[6] have shown that by heating the substrate over which the film flows, one can control the instabilities of the film. Shankar and Sahu,[7] Gaurav and Shankar[8] have shown that by taking the substrate as a deformable solid, one can suppress the perturbations of any wavelength at the free surface, by utilizing the elasto-hydrodynamic coupling between the liquid film and the solid deformation, without introducing any additional instability in the system. Blyth and Pozrikidis,[9] and Wei[10] have shown that the presence of an insoluble surfactant at the free surface of a thin film down an impermeable substrate suppresses the free surface instability and therefore this can be thought of as another strategy to control/suppress the free surface instability.

In fact, the Marangoni instability that arises due to the surface-tension driven convection in a pure fluid layer[11] has been considered by several investigators. One of the factors that can be important in the stability problems is the role of the surface-active agents and in view of this, the hydrodynamics of the surfactant has been addressed in the literature both from a fundamental and applied point of view. The convective motion of the surfactant leads to a heterogeneous surfactant distribution on the interface. Additional tangential stresses arise due to nonuniform distribution of the surfactant concentration which generates the surface-tension gradients and these have significant influence on convection. The investigations by Benjamin[12] and Whitaker[13] reveal that the presence of the surfactant at the surface of a film raises the critical Reynolds number for instability and hence stabilizes the film flow system. Whitaker and Jones[14] and Lin[15] have also shown that in the surfactant-laden flow of a film down an inclined plane, as the surfactant elasticity increases, the critical Reynolds number associated with the Yih-mode for a long-wave instability increases and that the role of the surfactant is to stabilize the film flow system. The analysis by Pozrikidis[16] on the stability of a film flow down a periodic wall in the presence of an insoluble surfactant for Stokes flow has shown the existence of a Marangoni normal mode whose rate of decay is lower than that of the usual mode for a clean surface. The study of the stability of a vertically falling film in the presence of a soluble surfactant by Ji and Setterwall[17] has revealed the existence of an unstable normal mode associated with the Marangoni stresses at small Reynolds numbers and for perturbations of short and moderate wavelengths.

There are also investigations on the effects of the surfactant on the stability of two-layer flows in confined channels. A linear stability analysis on a two-layer Couette-Poisuille channel flow[18,19] in the limit of long-waves, has revealed that a quiescent interface subjected to a local shear flow is unstable, due to periodic accumulation of the surfactant and the resulting spatial variations in the surface tension. The regions of instability in the parameter space of the ratio of viscosities and the layer thickness have been determined for Stokes flow by Halpern and Frankel[20] by extending the analysis of Frenkel and Halpern[18] to perturbations of arbitrary wavelength. Blyth and Pozrikidis[21] have considered the role of an insoluble surfactant on the interfacial stability of a two-layer viscous flow in an inclined channel confined by two parallel walls. The results of the linear stability analysis of a lubrication-flow model applicable to long-waves and low Reynolds number flow reveal the presence of the Marangoni instability in certain regions of the parameter space determined by the viscosity ratio and the layer thickness, thus confirming the results of Frenkel and Halpern[18] and Halpern and Frenkel.[19] In the subsequent investigations, Pozrikidis[22] and Blyth and Pozrikidis[23] have investigated the effects of inertia on the linear and nonlinear stages of instability. The structure and the dynamics of the film flow are influenced by the presence of the surfactant.

The investigations on the stability of a film down a porous inclined substrate, where a slip condition has been imposed at the substrate include the studies by Pascal,[24,25] Sadiq and Usha,[26] Sadiq, Usha, and Joo,[27] and Pascal and D'Alessio.[28] Pascal[24] has examined the linear stability of a thin Newtonian film down a permeable inclined plane which is modeled by the Navier-slip condition. The dimensionless slip coefficient accounts for the local geometry of the interface of the porous and the liquid layers. This one-domain model is based on the assumption that the superficial velocity in the porous medium is very small compared to the velocity in the liquid layer. Following the assumptions of Pascal,[24,25] there have been investigations on the stability of a Newtonian film flow down a permeable inclined substrate by Sadiq and Usha[26] (weakly nonlinear stability analysis

and evolution of nonlinear waves based on Benney's long wave expansion), Sadiq, Usha, and Joo[27] (heated porous substrate), and by Pascal and D'Alessio[28] (uneven surface). The results show that the effect of the slip coefficient is to destabilize the film flow system over a permeable substrate. Samanta *et al.*[29] have recently revisited the problem of a falling film down a slippery inclined plane within the framework of long-wave analysis and boundary layer approximations and have performed the linear stability analysis of the coupled depth-averaged equations derived for the local flow rate and the film thickness. They have observed that the effect of slip is to promote the onset of instability and thus has a destabilizing effect by lowering the critical Reynolds number. At larger Reynolds numbers, the effect is stabilizing. This effect has been observed for the cases, when the Reynolds number is based on the velocity at the free surface or the averaged velocity across the flow.

A slip condition at the substrate is a limiting form of a boundary condition at the interface of a fluid-porous medium. This suggests that an investigation on the stability of a flow of a thin film over a porous medium, by incorporating the momentum transport in the porous medium, might add additional information on the influence of the characteristics of the porous medium on the film above it. Further, in several practical applications, the bottom substrate is a porous substrate and a study of the dynamics of a thin film over a porous substrate gains significance in such applications. In view of this, Liu and Liu[30] have considered the Darcy model for the porous medium with Beavers-Joseph[31] boundary condition at the interface of the liquid and the porous layers and have examined the linear stability of a Newtonian film over it in the frame work of Orr-Sommerfeld analysis. The volume averaging technique developed by Whitaker[32] questions the validity of the Beavers-Joseph boundary condition at the interface of the porous/liquid layers and a stress-jump condition that accounts for the spatial heterogeneity of the interfacial region has been proposed.[33–36] Thiele *et al.*[37] have incorporated the momentum transport in the porous medium described by the Darcy-Brinkman equations[33,38,39] and the shear stress-jump condition (Whitaker[32]) at the interface of the porous and the liquid layers and have obtained the evolution equation for the film thickness based on Benney's[40] long-wave expansion. They have observed a destabilizing influence of the presence of the porous medium on the film flow system. An increase in the stress-jump co-efficient enhances this destabilizing effect.

The above investigation by Thiele *et al.*[37] and the results by Blyth and Pozrikidis,[9] on the stability of a thin film flow over an inclined impermeable substrate in the presence of an insoluble surfactant have motivated the present study in which the influence of the presence of an insoluble surfactant at the free surface of a thin film over an inclined porous substrate on the stability of the film flow system is examined. Such an investigation might also provide some information on the effects of the coupling of the forces due to the flow in the porous medium and the hydrodynamics of the contaminated film above it on the free surface instability, so that having the substrate as a porous medium rather than as an impermeable substrate can be thought of as another strategy to control or suppress the free surface instability.

The objective of the investigation is twofold: (i) to examine the linear stability of a clean film (Nusselt base flow) over a porous substrate incorporating the momentum transport in the porous medium with the stress-jump boundary condition at the interface, within the framework of Orr-Sommerfeld analysis and (ii) to investigate the above problem in the presence of an insoluble surfactant. It is of interest (a) to examine if the presence of the surfactant at the free surface suppresses the instability in a film over a porous substrate; (b) to find the range of parameters characterizing the porous medium for which the flow of a clean/contaminated film can be stabilized; and (c) to analyze the possibility of enhancing the instability of the film flow system outside the windows of stability for appropriate choices of the porous medium characteristics.

In view of the above, in this investigation, the stability of a gravity-driven flow of a thin viscous film over a porous substrate in the presence of an insoluble surfactant with surfactant concentration Γ at the air-film interface is considered. The general problem of a film over a porous substrate is formulated in Sec. II A; the base state solution corresponding to parallel uniform flow over a porous substrate is obtained in Sec. II B; using the stream function formulation, the Orr-Sommerfeld system of equations (PS) for the amplitudes of the perturbations in the stream-function, the surfactant concentration and the deflection of the free-surface are derived in Sec. II C. A linear stability analysis of the base state is performed in the long-wavelength limit and the effects of the presence of the

surfactant at the free surface are examined in Sec. II D. In Sec. II E, the Orr-Sommerfeld system (SS) is presented for the gravity-driven flow of a contaminated film over a slippery inclined substrate and the long-wavelength analysis of the system is performed. In Sec. III, the Orr-Sommerfeld systems (PS and SS) are solved numerically by the spectral-Tau collocation method and the solutions of the linear stability problem are presented for different parameter values governing the film flow system. From the results on the neutral stability curves in the wave number/Reynolds number space, it is observed that the presence of the surfactant has a stabilizing effect on the film flow system; the influence of the porous medium characteristics is interesting in the sense that by appropriate choice of the parameters governing the porous substrate such as the permeability, the porosity, the stress-jump coefficient, and the thickness of the porous layer, it is possible to find k-Re windows in which one can stabilize a clean/a contaminated film over a porous substrate as compared to such a film over a rigid substrate; further, outside these windows, it is possible to enhance the destabilizing effects of the porous medium on a clean/a contaminated film flow system.

II. MATHEMATICAL FORMULATION

A. The governing equations

A two-dimensional incompressible Newtonian fluid flowing over an inclined porous substrate saturated by the same liquid is considered (Fig. 1). The porous layer is of finite constant thickness d and is on a rigid wall, which is inclined at an angle θ to the horizontal as shown in Fig. 1. The surface of the film is occupied by an insoluble surfactant with surface concentration $\Gamma(x, t)$, which is convected. The surfactant diffuses freely over the film surface, but does not penetrate into the bulk of the fluid. The local surface tension $\sigma(x, t)$, at each point on the free surface, varies according to the local surfactant concentration. A linear relation between the surface tension and the surfactant concentration may be assumed, when the surfactant concentration is below the saturation level. It is, according to Gibbs, given by $\sigma_c - \sigma = \Gamma RT$, where R is the ideal gas constant, T is the absolute temperature, and σ_c is the surface tension of a clean interface that is devoid of surfactant.[41] This yields the linear equation of state $\sigma = \sigma_c(1 - \beta\frac{\Gamma}{\Gamma_0})$, where $\beta = \frac{\Gamma_0 RT}{\sigma_c}$ is a dimensionless constant related to the surface elasticity E employed in the surfactant literature by $E = \frac{\beta\sigma_c}{\Gamma_0}$, Γ_0 is a reference surfactant concentration. When the surfactant concentration has small variations around the reference value Γ_0, then, a Taylor expansion gives

$$\sigma = \sigma_0 - E(\Gamma - \Gamma_0). \tag{1}$$

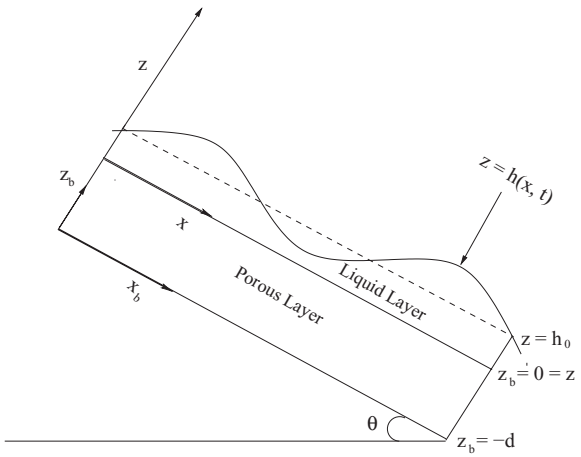

FIG. 1. Schematic diagram for a Newtonian film flow over a porous substrate.

The governing equations in the liquid film ($0 < z < h(x, t)$) are

$$u_x + w_z = 0, \tag{2}$$

$$u_t + uu_x + wu_z = -\frac{1}{\rho}p_x + \nu[u_{xx} + u_{zz}] + g\sin\theta, \tag{3}$$

$$w_t + uw_x + ww_z = -\frac{1}{\rho}p_z + \nu[w_{xx} + w_{zz}] - g\cos\theta, \tag{4}$$

where ρ, ν are the density and the kinematic viscosity of the fluid, respectively, u, w are the components of velocity in the x and z increasing directions, respectively, g is the acceleration due to gravity, and p is the pressure. The boundary conditions at the free surface $z = h(x, t)$ are the kinematic free-surface boundary condition, the balance of the tangential and the normal stresses given by

$$w = h_t + uh_x \text{ on } z = h(x, t), \tag{5}$$

$$\mu[-4u_xh_x + (u_z + w_x)(1 - h_x^2)] = \sigma_x(1 + h_x^2)^{\frac{1}{2}} \text{ on } z = h(x, t), \tag{6}$$

$$p = \frac{2\mu}{(1 + h_x^2)}[u_xh_x^2 - (u_z + w_x)h_x + w_z] - \frac{\sigma h_{xx}}{(1 + h_x^2)^{\frac{3}{2}}} \text{ on } z = h(x, t). \tag{7}$$

The momentum transport in the porous layer is described using the Darcy-Brinkman equations[33,38,39] given by

$$U_{x_b} + W_{z_b} = 0, \tag{8}$$

$$\frac{1}{\chi}U_{t_b} = -\frac{1}{\rho}P_{x_b} + \frac{\mu_e}{\rho}[U_{x_bx_b} + U_{z_bz_b}] + g\sin\theta - \frac{\nu}{K}U, \tag{9}$$

$$\frac{1}{\chi}W_{t_b} = -\frac{1}{\rho}P_{z_b} + \frac{\mu_e}{\rho}[W_{x_bx_b} + W_{z_bz_b}] - g\cos\theta - \frac{\nu}{K}W, \tag{10}$$

where (U, V) denote the filtration velocity components, K is the permeability, χ is the porosity, and μ_e is the effective viscosity (Whitaker[38]) and $\frac{\mu_e}{\mu} = \frac{1}{\chi}$. A subscript denotes the partial derivative with respect to that variable. The flow in the porous region is assumed to be slow enough to neglect inertia.[42] The theoretical development of the momentum transfer at the boundary between a porous medium and a homogeneous fluid described by Ochoa-Tapia and Whitaker[34] suggests the following conditions at the interface ($z = 0$) between the liquid layer and the porous layer. They are given by

$$u = U \text{ at } z = z_b = 0, \tag{11}$$

$$w = W \text{ at } z = z_b = 0, \tag{12}$$

$$\mu_eU_{z_b} - \mu u_z = \frac{\xi}{\sqrt{K}}U \text{ at } z = z_b = 0, \tag{13}$$

$$-P + 2\mu_eW_{z_b} = -p + 2\mu w_z \text{ at } z = z_b = 0. \tag{14}$$

Equations (11) and (12) correspond to the conditions for the continuity of velocity at the interface and Eq. (14) describes the continuity of the normal stress at the interface. Equation (13) represents a shear stress-jump condition at the interface, where the jump coefficient ξ accounts for the spatial heterogeneities of the interfacial region and depends on the characteristics of the continuous spatial variations of the effective properties like the porosity and the permeability of the porous layer. It represents a macroscopic description of the momentum transport in a finite mesoscopic interfacial transition layer. At the bottom of the porous substrate supported by a rigid wall,

$$U = 0 \text{ at } z_b = -d, \tag{15}$$

$$W = 0 \text{ at } z_b = -d. \tag{16}$$

The evolution of the surface surfactant concentration $\Gamma(x, t)$ is governed by[9,43]

$$\frac{\partial \Gamma}{\partial t} + \nabla_{\mathbf{s}}.(\Gamma \mathbf{u_s}) + \Gamma(\nabla_{\mathbf{s}}.\hat{\mathbf{n}})(\hat{\mathbf{u}}.\hat{\mathbf{n}}) = D_s \nabla_{\mathbf{s}}^2 \Gamma, \text{ on } z = h(x, t), \tag{17}$$

where $\nabla_{\mathbf{s}}.\hat{\mathbf{n}}$ is the mean curvature of the surface, $\nabla_{\mathbf{s}}$ is the surface gradient operator, $\nabla_{\mathbf{s}} = (\bar{\mathbf{I}} - \hat{\mathbf{n}}\hat{\mathbf{n}}).\nabla$, $\mathbf{\bar{u}_s}$ represents the velocity along the surface, $\mathbf{\bar{u}_s} = (\bar{\mathbf{I}} - \hat{\mathbf{n}}\hat{\mathbf{n}}).\bar{\mathbf{u}}$, $\hat{\mathbf{n}}$ is the local unit normal, $(\bar{\mathbf{u}}.\hat{\mathbf{n}})$ is the component of velocity along the normal to the surface, and D_s is the surface surfactant diffusivity. The dimensionless forms of Eqs. (1)–(17) are obtained using the following dimensionless variables:

$$\bar{x} = \frac{x}{h_0}, \quad \bar{z} = \frac{z}{h_0}, \quad \bar{t} = \frac{tV}{h_0}, \quad \bar{u} = \frac{u}{V}, \quad \bar{w} = \frac{w}{V}, \quad \bar{p} = \frac{p}{\rho V^2},$$
$$\bar{h} = \frac{h}{h_0}, \quad \bar{\Gamma} = \frac{\Gamma}{\Gamma_0}, \quad \bar{\sigma} = \frac{\sigma}{\sigma_0}, \bar{x_b} = \frac{x_b}{d}, \quad \bar{z_b} = \frac{z_b}{d}, \quad \bar{t_b} = \frac{t_b \nu}{d^2},$$
$$\bar{U} = \frac{Ud}{\nu}, \quad \bar{W} = \frac{Wd}{\nu}, \quad \bar{P} = \frac{Pd^2}{\rho \nu^2},$$

where h_0 is the mean film thickness of the fluid layer and V is the characteristic velocity scale. The characteristic velocity scale V for the fluid layer is chosen as the maximum velocity of a uniform Nusselt film on a rigid substrate (occurs at the free surface) given by $V = \frac{g h_0^2 sin\theta}{2\nu}$. The present study is motivated by the investigations by Liu and Liu,[30] Thiele *et al.*,[37] and Blyth and Pozrikidis[9] and hence, in order to compare the results with these investigations, the formulation is in terms of the Reynolds number based on the Nusselt film free surface velocity for a clean film over an impermeable substrate.[9,30,37] It is also noted that in the porous layer, the velocity scale related to the fluid viscosity ν (namely $\frac{\nu}{d}$) has been used (as in Thiele *et al.*,[37] Liu and Liu[30]).

The dimensionless governing equations and the boundary conditions (after suppressing the over bars) are obtained as

$$u_x + w_z = 0, \tag{18}$$

$$\mathrm{Re}[u_t + uu_x + wu_z] = -\mathrm{Re}p_x + [u_{xx} + u_{zz}] + \mathrm{GRe}, \tag{19}$$

$$\mathrm{Re}[w_t + uw_x + ww_z] = -\mathrm{Re}p_z + [w_{xx} + w_{zz}] - \mathrm{GRe}\cot\theta, \tag{20}$$

$$w = h_t + uh_x, \text{ on } z = h(x, t), \tag{21}$$

$$-4u_x h_x + (u_z + w_x)(1 - h_x^2) = -\frac{\mathrm{Ma}}{\mathrm{Ca}}\Gamma_x (1 + h_x^2)^{\frac{1}{2}}, \text{ on } z = h(x, t), \tag{22}$$

$$p = \frac{2}{\mathrm{Re}}\frac{1}{(1 + h_x^2)}[u_x h_x^2 - (u_z + w_x)h_x + w_z] - \frac{1}{\mathrm{Ca\,Re}}\frac{[1 - \mathrm{Ma}(\Gamma - 1)]h_{xx}}{(1 + h_x^2)^{\frac{3}{2}}}, \text{ on } z = h(x, t), \tag{23}$$

$$U_{x_b} + W_{z_b} = 0, \tag{24}$$

$$\frac{1}{\chi}U_{t_b} = -P_{x_b} + \frac{1}{\chi}[U_{x_b x_b} + U_{z_b z_b}] + \frac{\mathrm{G}}{\mathrm{Re}^2}\hat{d}^3 - \frac{U}{\delta^2}, \tag{25}$$

$$\frac{1}{\chi}W_{t_b} = -P_{z_b} + \frac{1}{\chi}[W_{x_b x_b} + W_{z_b z_b}] - \frac{\mathrm{G}}{\mathrm{Re}^2}\hat{d}^3\cot\theta - \frac{W}{\delta^2}, \tag{26}$$

$$u = \frac{\hat{d}}{\mathrm{Re}}U, \text{ at } z = z_b = 0, \tag{27}$$

$$w = \frac{\hat{d}}{\mathrm{Re}}W, \text{ at } z = z_b = 0, \tag{28}$$

$$\frac{1}{\chi}U_{z_b} - \frac{\mathrm{Re}}{\hat{d}^2}u_z = \frac{\lambda}{\delta}U, \text{ at } z = z_b = 0, \tag{29}$$

$$-p + \frac{2}{\mathrm{Re}}w_z = -\frac{\hat{d}^2}{\mathrm{Re}^2}P + \frac{2}{\chi}\frac{\hat{d}^2}{\mathrm{Re}^2}W_{z_b}, \text{ at } z = z_b = 0, \tag{30}$$

$$U = 0, \text{ at } z_b = -1, \tag{31}$$

$$W = 0, \text{ at } z_b = -1, \tag{32}$$

$$\frac{\partial \Gamma}{\partial t} + \nabla_{\mathbf{s}}.(\Gamma \mathbf{u_s}) + \Gamma(\nabla_{\mathbf{s}}.\hat{\mathbf{n}})(\hat{\mathbf{u}}.\hat{\mathbf{n}}) = D_s\nabla_{\mathbf{s}}^{\mathbf{2}}\Gamma, \text{ at } z = h(x,t), \tag{33}$$

where $\mathrm{Re} = \frac{Vh_0}{\nu}$ is the Reynolds number of the flow, $\mathrm{Ma} = \frac{E\Gamma_0}{\sigma_0}$ is the Marangoni number, $\mathrm{Ca} = \frac{\mu V}{\sigma_0}$ is the Capillary number, $\alpha = \frac{\sigma_0 h_0}{D_s \mu}$ is a dimensionless number related to the surfactant surface Péclet number $\mathrm{Pe} = \frac{h_0 V}{D_s} = \alpha \mathrm{Ca}$, $G = \frac{g h_0 sin\theta}{V^2}$ is the modified Galileo number, $\hat{d} = \frac{h_0}{d}$ is the ratio of mean film thickness of the liquid layer to the porous layer thickness, $\delta = \frac{\sqrt{K}}{d}$ is the Darcy number representing the dimensionless permeability of the porous medium, and $\lambda = \frac{\xi}{\mu}$ is the dimensionless stress-jump coefficient. In the following computations, $G \simeq O(1)$, χ is such that $0 < \chi < 1$ and $\lambda \simeq O(1)$, $\mathrm{Ma} = \mathrm{O}(1)$ and δ is such that $0 \leq \delta < \infty$.

B. The base flow

The equations and the boundary conditions corresponding to a plane-parallel flow of a thin Newtonian film with uniform film thickness over a porous substrate are given by Eqs. (A1)–(A11) in Appendix A and these are obtained from Eqs. (18)–(33). The solutions of (A1) and (A5) satisfying the boundary conditions are given by

$$u_B = [-\frac{\mathrm{GRe}z^2}{2} + \mathrm{GRe}z + \bar{M}], \tag{34}$$

$$U_B = C_1 e^{(\frac{-\sqrt{\chi}}{\delta})z_b} + C_2 e^{(\frac{\sqrt{\chi}}{\delta})z_b} + \frac{\mathrm{GRe}^2\delta^2}{\hat{d}^3}, \tag{35}$$

where

$$\bar{M} = \frac{\mathrm{GRe}\delta}{\hat{d}^2\Delta}[\delta(E_+ + E_- - 2) + \hat{d}\sqrt{\chi}(E_+ - E_-)],$$

$$C_1 = -\frac{\mathrm{GRe}^2\delta}{\hat{d}^3\Delta}[\delta B_- + (\delta\lambda + \hat{d})\sqrt{\chi}E_-],\ C_2 = -\frac{\mathrm{GRe}^2\delta}{\hat{d}^3\Delta}[\delta B_+ - (\delta\lambda + \hat{d})\sqrt{\chi}E_+],$$

$$\Delta = B_+E_- + B_-E_+,\ B_+ = 1 + \lambda\sqrt{\chi},\ B_- = 1 - \lambda\sqrt{\chi},\ E_+ = \exp(\tfrac{\sqrt{\chi}}{\delta}),\ E_- = \exp(\tfrac{-\sqrt{\chi}}{\delta}).$$

It is observed that the balance of stream-wise gravitational acceleration and the viscous forces has resulted in a parabolic velocity profile in the liquid layer. Since $\mathrm{GRe} = 2$, $u_B(1) = 1 + \bar{M}$, $u_B'(1) = 0$, $u_B''(1) = -2$.

C. The Orr-Sommerfeld eigenvalue problem

The stability of the base state (34)–(35) with respect to infinitesimal perturbations is considered. Substituting

$u(x,z,t) = u_B(z) + \tilde{u}(x,z,t)$, $w(x,z,t) = \tilde{w}(x,z,t)$, $p(x,z,t) = p_B(z) + \tilde{p}(x,z,t)$,
$U(x_b,z_b,t_b) = U_B(z_b) + \tilde{U}(x_b,z_b,t_b)$, $W(x_b,z_b,t_b) = \tilde{W}(x_b,z_b,t_b)$,
$P(x_b,z_b,t_b) = P_B(z_b) + \tilde{P}(x_b,z_b,t_b)$,
$h(x,t) = 1 + \tilde{h}(x,t)$, $\Gamma(x,t) = 1 + \tilde{\Gamma}(x,t)$,

into the equations of motion and the surfactant transport equation (18)–(33) and linearizing for $\tilde{u}$, $\tilde{w}$, $\tilde{U}$, $\tilde{W}$, $\tilde{p}$, $\tilde{P}$, $\tilde{h}, \tilde{\Gamma} \ll 1$, the equations for the perturbed quantities are

obtained as

$$\tilde{u}_x + \tilde{w}_z = 0, \tag{36}$$

$$\mathrm{Re}[\tilde{u}_t + u_B\tilde{u}_x + \tilde{w}u'_B] = -\mathrm{Re}\tilde{p}_x + [\tilde{u}_{xx} + \tilde{u}_{zz}], \tag{37}$$

$$\mathrm{Re}[\tilde{w}_t + u_B\tilde{w}_x] = -\mathrm{Re}\tilde{p}_z + [\tilde{w}_{xx} + \tilde{w}_{zz}], \tag{38}$$

$$\tilde{w} = \tilde{h}_t + u_B\tilde{h}, \text{ on } z = 1, \tag{39}$$

$$\tilde{h}u''_B = -\frac{\mathrm{Ma}}{\mathrm{Ca}}\tilde{\Gamma}_x - \tilde{u}_z - \tilde{w}_x, \text{ on } z = 1, \tag{40}$$

$$\mathrm{Re}\tilde{p} = \mathrm{GRe}\tilde{h}\ cot\theta + 2\tilde{w}_z - \frac{1}{\mathrm{Ca}}\tilde{h}_{xx}, \text{ on } z = 1, \tag{41}$$

$$\tilde{U}_{x_b} + \tilde{W}_{z_b} = 0, \tag{42}$$

$$\frac{1}{\chi}\tilde{U}_{t_b} = -\tilde{P}_{x_b} + \frac{1}{\chi}[\tilde{U}_{x_bx_b} + \tilde{U}_{z_bz_b}] - \frac{\tilde{U}}{\delta^2}, \tag{43}$$

$$\frac{1}{\chi}\tilde{W}_{t_b} = -\tilde{P}_{z_b} + \frac{1}{\chi}[\tilde{W}_{x_bx_b} + \tilde{W}_{z_bz_b}] - \frac{\tilde{W}}{\delta^2}, \tag{44}$$

$$\tilde{u} = \frac{\hat{d}}{\mathrm{Re}}\tilde{U}, \text{ at } z = z_b = 0, \tag{45}$$

$$\tilde{w} = \frac{\hat{d}}{\mathrm{Re}}\tilde{}, \text{ at } z = z_b = 0, \tag{46}$$

$$\frac{1}{\chi}\tilde{U}_{z_b} - \frac{\mathrm{Re}}{\hat{d}^2}\tilde{u}_z = \frac{\lambda}{\delta}\tilde{U}, \text{ on } z = z_b = 0, \tag{47}$$

$$-\tilde{p} + \frac{2}{\mathrm{Re}}\tilde{w}_z = -\frac{\hat{d}^2}{\mathrm{Re}^2}\tilde{P} + \frac{2}{\chi}\frac{\hat{d}^2}{\mathrm{Re}^2}\tilde{W}_{z_b}, \text{ on } z = z_b = 0, \tag{48}$$

$$\tilde{U} = 0, \text{ at } z_b = -1, \tag{49}$$

$$\tilde{W} = 0, \text{ at } z_b = -1, \tag{50}$$

$$\tilde{\Gamma}_t + \tilde{u}_x + \tilde{\Gamma}_x u_B = \frac{1}{\alpha\mathrm{Ca}}\tilde{\Gamma}_{xx}, \text{ on } z = 1. \tag{51}$$

Since the interface boundary conditions are evaluated at $z = 1 + \tilde{h}$, the boundary conditions (39)–(41) and (51) have been obtained using Taylor expansion at the undeformed free surface $h = 1$. The perturbation equations have been obtained in terms of $\tilde{w}$, $\tilde{\Gamma}$, and $\tilde{h}$ and are given by

$$\mathrm{Re}\left[\nabla^2\tilde{w}_t - u''_B\tilde{w}_x + u_B\nabla^2\tilde{w}_x\right] - \nabla^4\tilde{w} = 0, \tag{52}$$

$$\tilde{w} = \tilde{h}_t + u_B\tilde{h}_x, \text{ on } z = 1, \tag{53}$$

$$\mathrm{GRe}\ \cot\theta\tilde{h}_{xx} - \frac{\tilde{h}_{xxxx}}{\mathrm{Ca}} + 3\tilde{w}_{xxz} + \tilde{w}_{zzz} - \mathrm{Re}\tilde{w}_{zt} - \mathrm{Re}u_B(1)\tilde{w}_{xz} = 0, \text{ on } z = 1, \tag{54}$$

$$\tilde{h}_x u''_B = -\frac{\mathrm{Ma}}{\mathrm{Ca}}\tilde{\Gamma}_{xx} + \tilde{w}_{zz} - \tilde{w}_{xx}, \text{ on } z = 1, \tag{55}$$

$$\tilde{\Gamma}_t - \tilde{w}_z + \tilde{\Gamma}_x u_B = \frac{1}{\alpha\,\mathrm{Ca}}\tilde{\Gamma}, \text{ on } z = 1, \tag{56}$$

$$\frac{1}{\chi}\nabla_b^2[\nabla_b^2\tilde{W} - \tilde{W}_{t_b}] - \frac{\nabla_b^2\tilde{W}}{\delta^2} = 0, \tag{57}$$

$$u_B'\tilde{w}_x + \frac{3}{\mathrm{Re}}\tilde{w}_{xxz} + \frac{1}{\mathrm{Re}}\tilde{w}_{zzz} - \tilde{w}_{zt} - u_B\tilde{w}_{xz} - \frac{3}{\chi}\frac{\hat{d}^4}{\mathrm{Re}^2}\tilde{W}_{x_bx_bz_b} - \frac{1}{\chi}\frac{\hat{d}^4}{\mathrm{Re}^2}\tilde{W}_{z_bz_bz_b},$$
$$+ \frac{\hat{d}^4}{\mathrm{Re}^2\delta^2}\tilde{W}_{z_b} + \frac{\hat{d}^4}{\chi\mathrm{Re}^2}\tilde{W}_{z_bt_b} = 0, \text{ on } z = z_b = 0, \tag{58}$$

$$\frac{\hat{d}^3}{Re\chi}\tilde{W}_{z_bz_b} - \tilde{w}_{zz} = \frac{\lambda}{\delta}\frac{\hat{d}^3}{\mathrm{Re}}\tilde{W}, \text{ on } z = z_b = 0, \tag{59}$$

$$\tilde{w}_z = \frac{\hat{d}^2}{\mathrm{Re}}\tilde{W}_{z_b}, \text{ on } z = z_b = 0, \tag{60}$$

$$\tilde{w} = \frac{\hat{d}}{\mathrm{Re}}\tilde{W}, \text{ on } z = z_b = 0, \tag{61}$$

$$\tilde{W}_{z_b} = 0, \text{ on } z_b = -1, \tag{62}$$

$$\tilde{W} = 0, \text{ on } z_b = -1. \tag{63}$$

Note that $D_b = \frac{d}{dz_b} = \frac{1}{\hat{d}}\frac{d}{dz} = \frac{1}{\hat{d}}D$, $\hat{d}z = z_b$, $\hat{d}x = x_b$, $t = \frac{\mathrm{Re}}{\hat{d}^2}t_b$.

Using the stream functions $\tilde{\psi}$, $\tilde{\psi}^b$ where $\tilde{u} = \tilde{\psi}_z$, $\tilde{w} = -\tilde{\psi}_x$, $\tilde{U} = \tilde{\psi}^b_{z_b}$, $\tilde{W} = -\tilde{\psi}^b_{x_b}$ and seeking solutions of (52)–(63) in the form of normal modes $\tilde{\psi}(x,z,t) = \phi(z)e^{ik(x-ct)}$, $\tilde{\psi}^b(x_b,z_b,t_b) = \phi^b(z_b)e^{ik_b(x_b-c_bt_b)}$, $\tilde{h}(x,t) = \tilde{\zeta}e^{ik(x-ct)}$, $\tilde{\Gamma}(x,t) = \Gamma_* e^{ik(x-ct)}$ where k, k_b are wave numbers ($k = \hat{d}k_b$) c, c_b are the complex wave velocities ($c = \frac{\hat{d}}{\mathrm{Re}}c_b$), the Orr-Sommerfeld system is obtained as

$$(D^2 - k^2)^2\phi - \mathrm{Re}\Big[ik(u_B - c)(D^2 - k^2)\phi - iku_B''\phi\Big] = 0, \tag{64}$$

$$\phi + \tilde{\zeta}(u_B - c) = 0, \text{ on } z = 1, \tag{65}$$

$$-ikD^3\phi + \Big[\mathrm{Re}k^2(c - u_B) + 3ik^3\Big]D\phi - \Big[\mathrm{GRe}k^2\cot\theta + \frac{k^4}{\mathrm{Ca}}\Big]\tilde{\zeta} = 0, \text{ on } z = 1, \tag{66}$$

$$u_B''\tilde{\zeta} + \frac{ik\mathrm{Ma}}{\mathrm{Ca}}\Gamma_* + D^2\phi + k^2\phi = 0, \text{ on } z = 1, \tag{67}$$

$$\phi' + \Gamma_*\Big[(u_B - c) - \frac{ik}{\alpha\mathrm{Ca}}\Big] = 0, \text{ on } z = 1, \tag{68}$$

$$\Big[1 - \frac{ikc\mathrm{Re}\delta^2}{\hat{d}^2\chi} - \frac{\delta^2}{\chi}({D_b}^2 - \frac{k^2}{\hat{d}^2})\Big]\Big[{D_b}^2 - \frac{k^2}{\hat{d}^2}\Big]\phi^b = 0, \tag{69}$$

$$\mathrm{Re}\Big[u_B'ik\phi - ik(u_B - c)D\phi\Big] + (D^3 - 3k^2D)\phi$$
$$= \frac{\hat{d}^3}{\mathrm{Re}}\Big[\frac{1}{\chi}({D_b}^3 - 3\frac{k^2}{\hat{d}^2}D_b)\phi^b - \frac{1}{\delta^2}D_b\phi^b + \frac{ikc\mathrm{Re}}{\hat{d}^2\chi}D_b\phi^b\Big], \text{ on } z = z_b = 0, \tag{70}$$

$$\mathrm{Re}\phi = \phi^b, \text{ on } z = z_b = 0, \tag{71}$$

$$\mathrm{Re}D\phi = \hat{d}D_b\phi^b, \text{ on } z = z_b = 0, \tag{72}$$

$$D^2\phi - \frac{\hat{d}^2}{\mathrm{Re}\chi}{D_b}^2\phi^b = -\frac{\lambda\hat{d}^2}{\delta\mathrm{Re}}D_b\phi^b, \text{ on } z = z_b = 0, \tag{73}$$

$$D_b\phi^b = 0, \text{ on } z_b = -1, \tag{74}$$

$$\phi^b = 0, \text{ on } z_b = -1. \tag{75}$$

Equations (64)–(75) describe a generalized eigenvalue problem and the values of the parameter $c = c_r + is$ for which a non-trivial solution exists are obtained. Here, c_r denotes the wave speed and s is the growth rate. When the bottom substrate is taken as an impermeable substrate, (i) the above system, in the absence of an insoluble surfactant at the free surface, reduces to the Orr-Sommerfeld equations for a Newtonian flow down an impermeable inclined substrate given by Yih[44] and Olsson and Henningson;[45] (ii) in the presence of an insoluble surfactant, the system reduces to that derived by Blyth and Pozrikidis.[9]

D. Long-wavelength stability analysis

A linear stability analysis of the base state (Eqs. (34) and (35)) is performed in the limit of long-wavelength ($k \to 0$), by following the regular perturbation technique proposed by Yih[44] and Benjamin[46] for the case of a contaminated film over a porous substrate. According to long-wave analysis, the amplitudes of the perturbations $\phi(z)$, $\phi^b(z_b)$, $\tilde{\zeta}$, Γ_*, and c are expanded in powers of the wave number k as

$$\phi = \phi_0 + k\phi_1 + O(k^2), \tag{76}$$

with similar expansions for the other variables. Substituting the above in the Orr-Sommerfeld equations and the boundary conditions (64)–(75) and collecting the terms at O(1), the zeroth order equations and the boundary conditions are obtained (Eqs. (B1)–(B12) in Appendix B). The solutions to (B1) and (B7) satisfying the boundary conditions are given by

$$\phi_0 = A_2\frac{z^2}{2} + A_3 z + A_4, \tag{77}$$

$$\phi_0^b = B_1 + B_2 e^{\sqrt{p}z_b} + B_3 e^{-\sqrt{p}z_b}, \tag{78}$$

where

$$A_2 = 2\zeta_0,\ A_3 = \frac{2\delta\sqrt{\chi}}{\hat{d}}\frac{(E_+ - E_-)\zeta_0}{\Delta},$$

$$A_4 = \frac{2\delta^2}{\hat{d}^2}\frac{(E_+ + E_- - 2)\zeta_0}{\Delta},$$

$$p = \frac{\chi}{\delta^2},\ B_1 = \frac{2\mathrm{Re}\delta^2}{\hat{d}^2}\frac{u_B''(1)\zeta_0}{\Delta},\ B_2 = -\frac{\mathrm{Re}\delta^2}{\hat{d}^2}\frac{u_B''(1)\zeta_0 E_+}{\Delta},\ B_3 = -\frac{\mathrm{Re}\delta^2}{\hat{d}^2}\frac{u_B''(1)\zeta_0 E_-}{\Delta}.$$

Substitution of (77) in (B2) and (B5) yields

$$\Big[c_0 - u_B(1)\Big]\zeta_0 = \phi_0(1), \tag{79}$$

$$\Big[c_0 - u_B(1)\Big]\Gamma_0 = -u_B''(1)\Big[1 + \frac{\delta\sqrt{\chi}}{\hat{d}}\frac{(E_+ - E_-)}{\Delta}\Big]\zeta_0. \tag{80}$$

There are two modes, namely, the Yih mode-associated with the interfacial deflection and the surfactant mode-associated with the presence of the surfactant. For $\zeta \neq 0$ (interface mode), c_0 and Γ_0 are given by

$$c_0 = 2(1 + \bar{M}), \tag{81}$$

$$\Gamma_0 = \frac{2\zeta_0}{1 + \bar{M}}\Big[1 + \frac{\delta\sqrt{\chi}}{\hat{d}}\frac{(E_+ - E_-)}{\Delta}\Big]. \tag{82}$$

It is observed from (81) that the long waves travel at twice the surface velocity and that it depends on the porous medium characteristics. The surface velocity for a film over a porous substrate is more than that for a film over an impermeable substrate. Equation (82) reveals that, at this order, the surfactant concentration perturbation is in phase with the interfacial deflection. This means that the surfactant concentration is higher(lower) at the interface's crest(trough). As a result of the gradient in surfactant concentration, Marangoni stresses are generated which push the fluid away from the crest and pull it towards the trough. This indicates that at this leading order, free surface deflections are suppressed.

In addition to the Yih mode, there is a surfactant mode that is associated with the surfactant concentration perturbation ($\Gamma_0 \neq 0$). For this mode

$$\zeta_0 = 0,$$

$$\Big[c_0 - u_B(1)\Big]\Gamma_0 = 0, \tag{83}$$

which gives $c_0 = 1+\bar{M}$ as $\Gamma_0 \neq 0$.

The solutions to the equations at O(k) given by (B13) and (B18) in Appendix B, satisfying the boundary conditions are given by

$$\phi_1 = 2i\mathrm{Re}\Gamma_0\Big[u_B(1) - c_0\Big]\Big[-\frac{1}{120}z^5 + \frac{1}{24}z^4\Big] + \frac{a_1}{6}z^3 + \frac{a_2}{2}z^2 + a_3 z + a_4, \tag{84}$$

$$\phi_1^b = b_1 e^{\sqrt{p}z_b} + b_2 e^{-\sqrt{p}z_b} + b_3 z_b + b_4 - \frac{ic_0\mathrm{Re}\delta}{2\hat{d}^2\sqrt{\chi}}\Big[B_3 e^{\sqrt{p}z_b} - B_4 e^{-\sqrt{p}z_b}\Big]z_b, \tag{85}$$

where a_i, b_i, $i = 1$ to 4, A and K are as in (B25) in Appendix B. Substituting (84), (85) and (B25) in (B14), the wave speed at the first order is determined as

$$\begin{aligned} c_1 = -i\cot\theta\Big[\frac{2}{3} + \frac{2\delta\sqrt{\chi}}{\hat{d}}\frac{(E_+ - E_-)}{\Delta} + \frac{2\delta^2}{\hat{d}^3}\Big(1 - \frac{\delta}{\sqrt{\chi}}\frac{(E_+ - E_-)}{\Delta}\Big) + \frac{4\delta^2}{\hat{d}^3\Delta}(E_+ + E_- - 2)(\lambda\delta + \hat{d})\Big] \\ - \frac{i\mathrm{Ma}}{\mathrm{Ca}}\Big[1 + \frac{\delta\sqrt{\chi}}{\hat{d}}\frac{(E_+ - E_-)}{\Delta}\Big] + i\mathrm{Re}\Big[\Big(\frac{8}{15} + \frac{4}{3}\bar{M} + \bar{M}^2\Big)\Big(1 + \frac{\delta\sqrt{\chi}}{\hat{d}}\frac{(E_+ - E_-)}{\Delta}\Big) \\ - \frac{2(1+\bar{M})\delta^3}{\hat{d}^3\sqrt{\chi}}\frac{(E_+ - E_-)}{\Delta} - \frac{4(1+\bar{M})\delta^3}{\hat{d}^4\sqrt{\chi}\Delta^2}\Big(\frac{2\hat{d}\sqrt{\chi}}{\delta} - \lambda\sqrt{\chi}(E_+ + E_- - 2) + (E_+ - E_-)\Big) \\ + \frac{\bar{M}(1+\bar{M})\delta^2}{\hat{d}^2\Delta}\Big(\frac{2}{\chi}(E_+ + E_-) - \frac{\lambda}{\sqrt{\chi}}(E_+ - E_-)\Big)\Big]. \end{aligned} \tag{86}$$

In the absence of the porous substrate, (86) reduces to the asymptotic solution obtained by Blyth and Pozrikidis.[9] In the absence of the surfactant (Ma = 0), the results of Benjamin[46] and Yih,[44] confirmed by the experimental results by Liu *et al.*[47] are recovered. The first term arises due to the transverse component of gravity, the second term appears as a result of the presence of an insoluble surfactant at the interface and the last term appears due to the inertial effects. Further, the expressions for the speed of the small amplitude surface waves given by c_0 (Eq. (81)) and the growth rate c_1 (Eq. (86)) are analogous to those presented by Thiele *et al.*[37] for the isothermal problem in the absence of an insoluble surfactant at the free surface (differences in the expressions are due to the choice of scales for the variables).

E. Contaminated film over a slippery inclined substrate: Long-wavelength analysis

By a film over a slippery inclined substrate, it is meant that a liquid film is flowing down a saturated porous substrate which is modeled by an impermeable substrate (say at $z = 0$) with a Navier-slip boundary condition $u = \frac{\sqrt{K}}{\alpha}u_z$ (dimensional variables) at the substrate z = 0. Here, α is the empirical dimensionless parameter appearing in the Beavers-Joseph boundary condition. Such a modeling is valid when the superficial velocity in the porous medium is small in comparison to the

fluid velocity above the porous medium.[25,26] As mentioned in the Introduction, this model has been used in a number of investigations[24–29] and the effects of slip on the stability of the film flow system have been examined.

In this section, the Orr-Sommerfeld system is derived for a gravity-driven film on a slippery inclined substrate in the presence of an insoluble surfactant and the long-wavelength analysis is performed. The Orr-Sommerfeld system in this case reduces to Eqs. (64)–(68) along with the boundary conditions

$$\phi = 0, \text{ on } z = 0, \tag{87}$$

$$\phi' = \beta\phi'', \text{ on } z = 0, \tag{88}$$

where $\beta = \frac{\sqrt{K}}{\alpha h_0}$ is the dimensionless slip length. A long-wavelength analysis similar to that described in Sec. II D is performed and the results show that there are two modes, namely, the Yih/the interface mode and the Marangoni mode. For the interface mode, the wave speed and the surfactant concentration at the leading order are given by

$$c_0 = 2(1 + 2\beta), \tag{89}$$

$$\Gamma_0 = \frac{2\zeta_0}{1 + 2\beta}[1 + \beta]. \tag{90}$$

For the surfactant mode,

$$\zeta_0 = 0,$$

$$c_0 = 1 + 2\beta. \tag{91}$$

From the solution at O(k), the growth rate c_1 for the interface mode is obtained as

$$c_1 = -(\frac{2}{3} + 2\beta)i\cot\theta - (1 + \beta)i\frac{\text{Ma}}{\text{Ca}} + \frac{4}{15}i\text{Re}\left[2 + 10\beta + 15\beta^2\right](1 + \beta). \tag{92}$$

Comparison of Eqs. (89), (90), and (92) with Eqs. (81), (82), and (86) shows that the expressions in the leading order terms (up to terms proportional to dimensionless slip length) are identical, when the dimensionless slip length β is identified with $\frac{\delta\sqrt{\chi}}{\hat{d}}\frac{(E_+ - E_-)}{\Delta}$, which again represents a dimensionless length expressed in terms of the porous medium characteristics. From Eq. (92), it is observed that the transverse component of gravity and the presence of surfactant tend to stabilize, while the inertial effects tend to destabilize the system.

In what follows, the equations (PS) given by (64)–(75) are solved numerically and the parameter regimes of flow instability are determined. Further, the Orr-Sommerfeld system (SS) for the contaminated film flow over a slippery inclined plane (Eqs. (64)–(68), (87), and (88)) is also solved numerically and the results of this one-domain model are compared with the results of the Orr-Sommerfeld system (PS).

III. NUMERICAL RESULTS

A spectral-Tau collocation method based on Chebyshev polynomials is used for discretizing the generalized eigenvalue problem described by Eqs. (64)–(75).[45] The solution of this system yields complex phase velocity $c = c_r + is$, from which the dimensionless growth rate s is obtained. The range of k (wave number) for which $s > 0$ is determined. The accuracy of the eigenvalues is tested by varying the number of polynomials used in the computation and the spurious eigenvalues are eliminated in the process. In order to validate the code employed in the computations, the numerical results for the growth rate of a clean film over an impermeable inclined substrate ($\theta = 4^\circ$) have been obtained for Re = 2500 (Ma = 0, solid curve, Fig. 2(a) in this paper) and the results agree with those presented by Blyth and Pozrikidis (Fig. 3 in Blyth and Pozrikidis[9]) and by Chin *et al.* (Fig. 5 in Chin *et al.*[48]). Based on the confidence gained by the accuracy of the above results, the developed code has been used to compute the results for a clean/contaminated film over an impermeable/porous

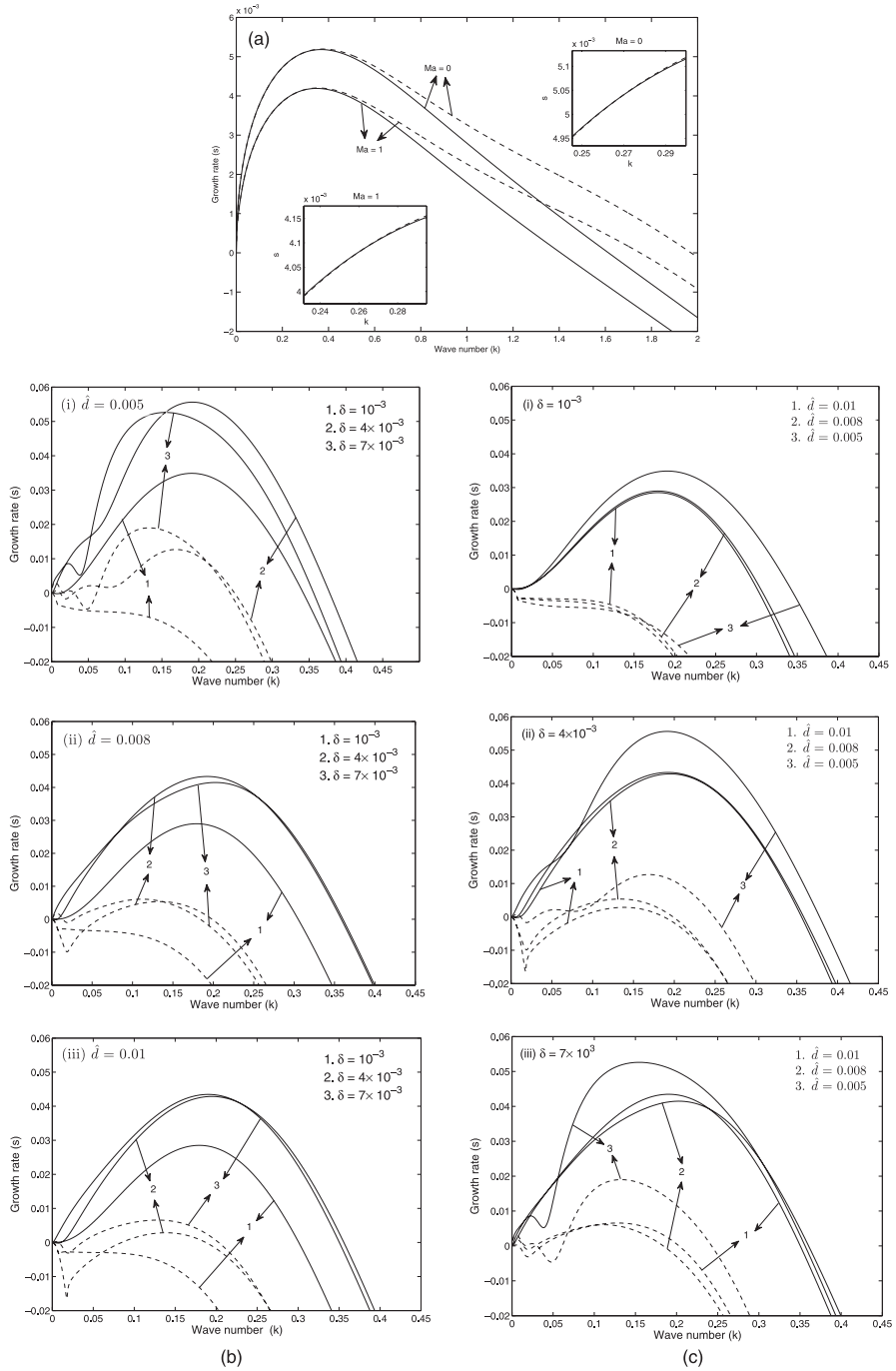

FIG. 2. (a) The growth rate of the dominant mode as a function of wave number when $\theta = 4^\circ$, Ca $= 0.017716$, $\alpha = 1$, and Re $= 2500$ for a film over an impermeable substrate (solid curve) and over a porous substrate (dashed curve) with $\hat{d} = 0.01$, $\chi = 0.1$, $\lambda = 0$, and $\delta = 10^{-3}$. (b) The growth rate of the dominant mode as a function of wave number for different $\hat{d}$ values, when $\theta = 45^\circ$, Ca $= 0.017716$, $\alpha = 1$, and Re $= 6$, for a clean (Ma $= 0$; solid curve)/a contaminated film (Ma $= 1$; dashed curve) over a porous substrate with $\lambda = 0$ and $\chi = 0.1$. (c) The growth rate of the dominant mode as a function of wave number for different Darcy number δ, when $\theta = 45^\circ$, Ca $= 0.017716$, $\alpha = 1$ and Re $= 6$, for a clean (Ma $= 0$; solid curve)/a contaminated film (Ma $= 1$; dashed curve) over a porous substrate with $\lambda = 0$ and $\chi = 0.1$.

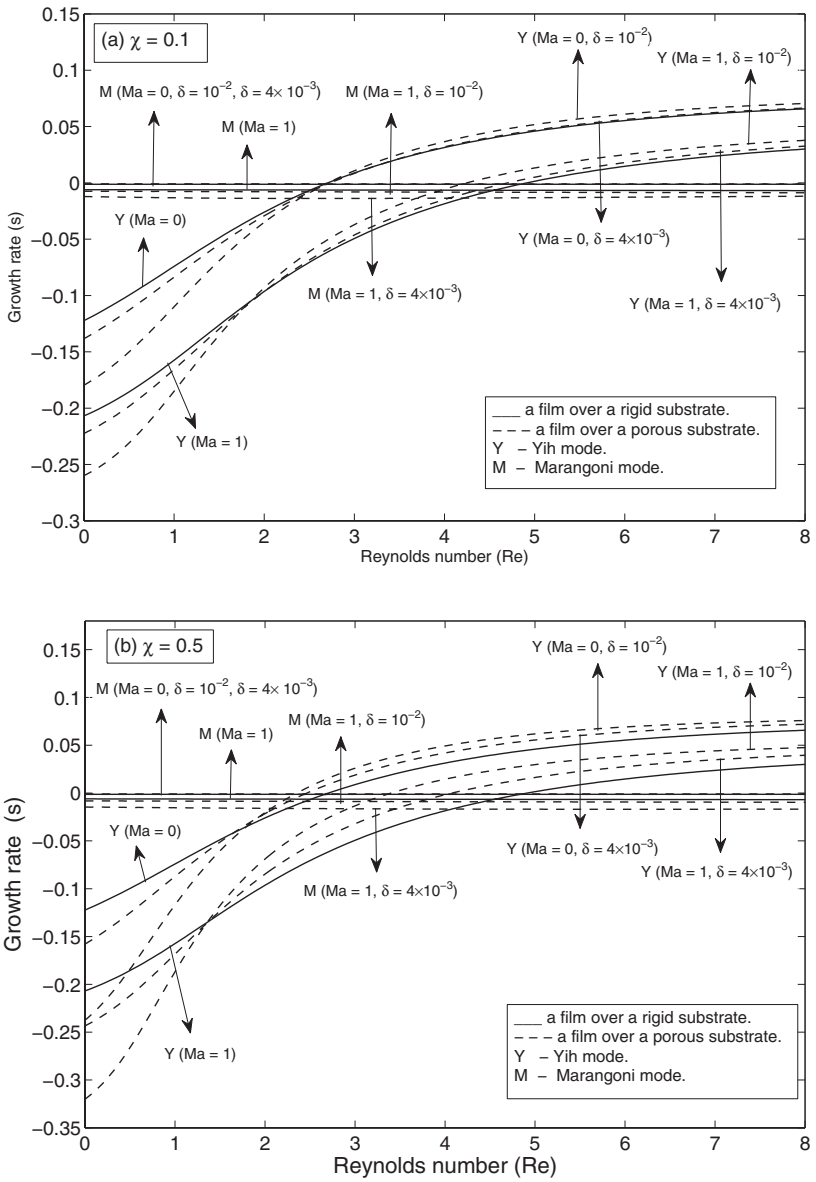

FIG. 3. (a) Effects of inertia on the growth rates when $k = 0.5$, $\alpha = 100$, and Ca = 2, for different values of the Darcy number δ with $\lambda = 0$, $\hat{d} = 0.05$, and $\chi = 0.1$. (b) Effects of inertia on the growth rates as the Darcy number δ varies when $\chi = 0.5$, for $\lambda = 0.5$, $\hat{d} = 0.05$ and $k = 0.5$, $\alpha = 100$, and Ca = 2.

substrate. The effects of the characteristics of the porous layer such as the ratio of the thickness of the liquid layer to the porous layer ($\hat{d}$), the porosity (χ), the Darcy number (δ), the stress-jump coefficient (λ) on the growth rate, and the stability of the film are examined. In what follows, a clean film is identified with Ma = 0 and a contaminated film with Ma = 1.

Figure 2(a) shows the growth rate (s) of the most dangerous mode as a function of the wave number (k) for a clean (Ma = 0) and a contaminated film (Ma = 1), when the Darcy number $\delta = 10^{-3}$ and the thickness parameter $\hat{d} = 0.01$. The other parameters are taken as $\chi = 0.1$, $\lambda = 0$, and $\alpha = 1$. The results for a film over an impermeable (porous) substrate are represented by solid

(dashed) curves, respectively. As k increases, the growth rate initially increases, attains a maximum, and then it decays. The maximum growth rate is slightly increased for a clean/a contaminated film over a porous substrate (inset figures, dashed lines). Beyond a certain k, where the growth rate attains its maximum, the growth rate of a contaminated film over an impermeable/a porous substrate is less than that of a clean film. This indicates that the presence of the surfactant at the free surface tends to suppress the growth rate of a contaminated film over an impermeable/a porous substrate. Also, beyond a certain k, the effect of the presence of the porous substrate is to enhance the growth rate of a clean/a contaminated film over it. Further, the range of k where the growth rate is positive for a clean/a contaminated film over a porous substrate is larger than that over an impermeable substrate.

Figure 2(b) presents the growth rate of the dominant mode for a film over a porous substrate for three different values of the dimensionless thickness parameter $\hat{d}$ ($\hat{d} = 0.005$ in (i), $\hat{d} = 0.008$ in (ii), and $\hat{d} = 0.01$ in (iii)). The figure shows the effects of the Darcy number δ on the growth rate at each $\hat{d}$ value considered. The other parameters are fixed at $\theta = 45^\circ$, $\lambda = 0$, $\chi = 0.1$, $\alpha = 1$, and $\mathrm{Ca} = 0.017716$. Here, the results for a clean film over a porous substrate (a contaminated film over a porous substrate) are represented by solid (dashed) curves, respectively.

In the case of a clean film (solid curves 1, 2, and 3 in Fig. 2(b) (i), (ii), and (iii)), the growth rate for the Darcy number $\delta = 10^{-3}$ (solid curve 1) is less than that for the other values of δ considered (solid curves 2 and 3). The growth rate for $\delta = 7 \times 10^{-3}$ is more than that for $\delta = 4 \times 10^{-3}$ up to a certain k, and beyond this k, the trend is reversed (solid curves 2, 3 in Fig. 2(b) (i), (ii), and (iii)). For a fixed wave number k, the growth rate is more for a thicker porous layer ($\hat{d} = 0.005$, Fig. 2(b) (i)) for the values of δ considered.

The growth rate for a contaminated film over a porous substrate with Darcy number $\delta = 7 \times 10^{-3}$ (dashed curve 3 in Fig. 2(b) (i), (ii), and (iii)) is more than that for the other values of the Darcy numbers considered. For a fixed k, the growth rate of a contaminated film over a thicker porous layer (Fig. 2(b) (i), dashed curve 3 for $\hat{d} = 0.005$, $\delta = 7 \times 10^{-3}$) is more than that for $\hat{d} = 0.008$ and $\hat{d} = 0.01$ when $\delta = 7 \times 10^{-3}$ (Fig. 2(b) (ii), dashed curves for $\hat{d} = 0.008$, $\delta = 7 \times 10^{-3}$ and $\hat{d} = 0.01$, $\delta = 7 \times 10^{-3}$). The results show that the growth rate of a clean/a contaminated film over a porous substrate is more when it flows over a thicker porous layer.

Figure 2(c) presents the growth rate of the dominant mode for a film over a porous substrate, for three different values of the Darcy number δ ($\delta = 10^{-3}$ in Fig. 2(c) (i); $\delta = 4 \times 10^{-3}$ in Fig. 2(c) (ii); and $\delta = 7 \times 10^{-3}$ in Fig. 2(c) (iii)). It shows the effects of the dimensionless porous layer thickness ($\hat{d}$) on the growth rate at each δ considered. The other parameter values are taken as $\theta = 45^\circ$; $\mathrm{Ca} = 0.017716$, $\mathrm{Re} = 6$, $\lambda = 0$, $\chi = 0.1$, and $\alpha = 1$. Here, the solid (dashed curves) represent the results for a clean (a contaminated) film over a porous substrate, respectively. The growth rate increases with a decrease in $\hat{d}$ for $\delta = 10^{-3}$ and $\delta = 4 \times 10^{-3}$ as in Fig. 2(c) (i) and (ii). It exhibits a non-monotonic behaviour for $\delta = 7 \times 10^{-3}$ (Fig. 2(c) (iii)). It is observed from Fig. 2(c) (i) ($\delta = 10^{-3}$) that the growth rate is negative for a contaminated film (dashed curves 1, 2, 3) for $\hat{d} = 0.008$, $\hat{d} = 0.005$ and $\hat{d} = 0.01$. As δ increases, the growth rate becomes positive beyond a certain small k (Fig. 2(c) (ii) and (iii)). After this k, the growth rate increases with a decrease in $\hat{d}$ for $\delta = 4 \times 10^{-3}$ (Fig. 2(c) (ii)), dashed curves 1, 2, 3) and exhibits a non-monotonic behaviour for $\delta = 7 \times 10^{-3}$ (Fig. 2(c), dashed curves 1, 2, 3).

The results from Fig. 2(c) show that the growth rate of a clean/a contaminated film over a porous substrate is maximum for a thicker porous layer and this is observed for all the Darcy numbers considered in this investigations.

Figure 3 presents the effects of inertia on the growth rates of the Yih and the Marangoni modes for a clean/a contaminated film over an impermeable/a porous substrate. The effects of permeability are analyzed for $\hat{d} = 0.05$, $\lambda = 0$, $\mathrm{Ca} = 2$, and $\theta = 45^\circ$ when $k = 0.5$ (Fig. 3(a); $\chi = 0.1$, $\lambda = 0$) and (Fig. 3(b); $\chi = 0.5$, $\lambda = 0.5$). The results for a film over an impermeable substrate are represented by thick solid curves and that over a porous substrate by dashed curves. The notation Y(Ma = 0) and Y(Ma = 1) denote the results for the Yih mode for a clean and a contaminated film over an impermeable substrate, respectively, and Y(Ma = 0, δ), Y(Ma = 1, δ) denote the corresponding results for a clean and a contaminated film over a porous substrate with Darcy number δ. Similar notations are used to represent the Marangoni mode so that M (Ma = 1) corresponds to the results for the Marangoni mode for a contaminated film over an impermeable substrate and M (Ma = 0,

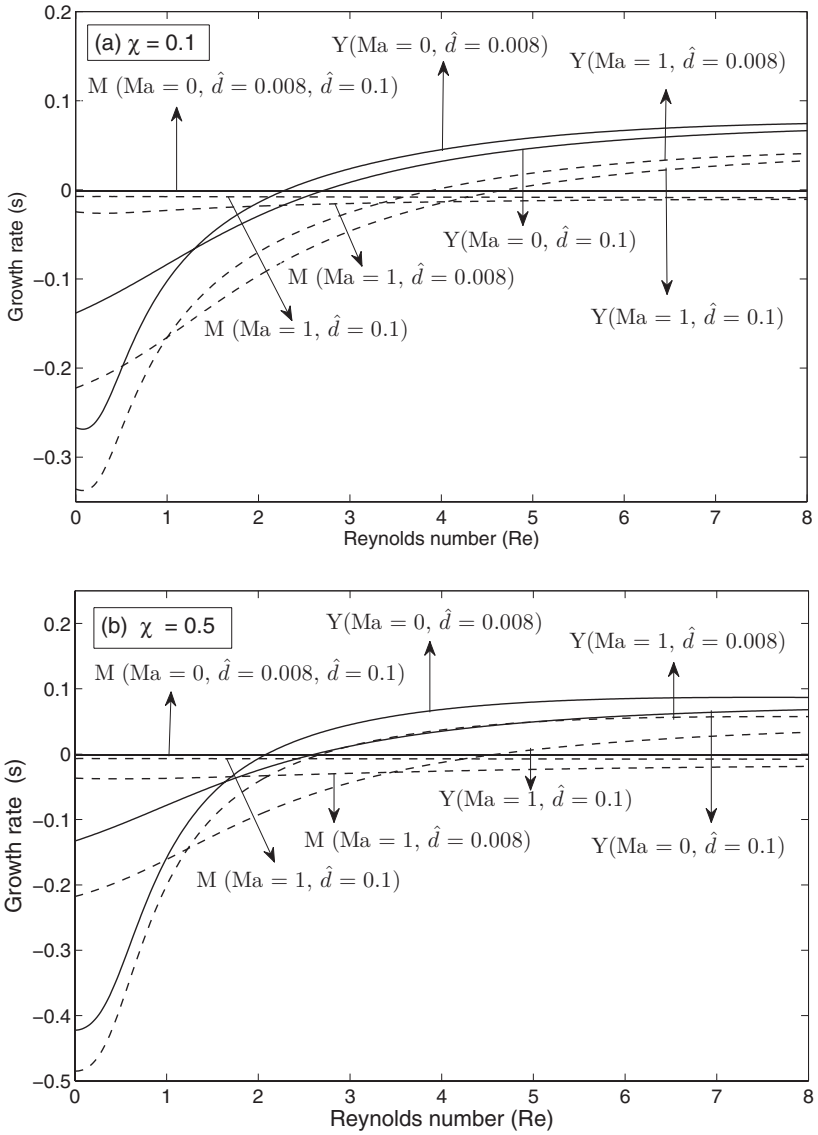

FIG. 4. Effects of inertia on the growth rates for a film over a porous substrate for different values of the thickness parameter $\hat{d}$, when k = 0.5, $\alpha = 100$, Ca = 2, $\lambda = 0$, and $\delta = 4 \times 10^{-3}$. (a) $\chi = 0.1$, (b) $\chi = 0.5$.

δ) and M (Ma = 1, δ) denote the results for the Marangoni mode for a clean and a contaminated film over a porous substrate with Darcy number δ. The curve described by (Ma = 0, $\delta = 10^{-2}$, $\delta = 4 \times 10^{-3}$ in Fig. 3(a)) shows that the results of the Marangoni mode for a clean film over an impermeable substrate and the results on a porous substrate with Darcy numbers $\delta = 10^{-2}$, $\delta = 4 \times 10^{-3}$ are very close to each other. The results for Y(Ma = 0) over an impermeable substrate agrees with the results obtained by Yih[44] and Blyth and Pozrikidis.[9] Also the results Y(Ma = 1) and M(Ma = 1) for a contaminated film over an impermeable substrate agree with those presented by Blyth and Pozrikidis[9] (Fig. 4(a) in their paper for $Re \neq 0$) and Pozrikidis[22] (for Re = 0).

It is observed from Figs. 3(a) and 3(b) that the Marangoni mode dominates only when the Reynolds number is sufficiently small. There is an increase in the growth rate of the Yih mode with an increase in the Reynolds number. As the Reynolds number is further increased, the growth rate

TABLE I. Critical Reynolds number values for different values of χ when $\lambda = 0$, Ca $= 2$, $\alpha = 1$, $\theta = 45^\circ$.

		$\hat{d} = 0.01$			$\hat{d} = 0.05$			$\hat{d} = 0.1$		
$\downarrow\delta$	$\chi \rightarrow$	0.1	0.2	0.5	0.1	0.2	0.5	0.1	0.2	0.5
4×10^{-3}	Ma $= 0$	4.111	4.791	4.511	1.531	1.491	1.391	1.251	1.231	1.191
	Ma $= 1$	4.251	4.951	4.671	2.331	2.231	2.071	2.131	2.091	2.011
7×10^{-3}	Ma $= 0$	1.571	2.211	2.791	1.991	1.891	1.671	1.331	1.291	1.211
	Ma $= 1$	1.591	2.251	2.831	2.651	2.511	2.211	2.131	2.071	1.931
1×10^{-2}	Ma $= 0$	0.631	0.971	1.431	2.331	2.251	1.931	1.411	1.351	1.251
	Ma $= 1$	0.631	0.971	1.451	2.851	2.731	2.351	2.171	2.071	1.891

of the Yih mode passes through the zero value and at the corresponding Reynolds number, there is an exchange of stability and the film flow becomes unstable and the Yih mode becomes dominant from then on. On the other hand, there is hardly any change in the growth rate of the Marangoni mode as the Reynolds number is increased and the corresponding perturbations remain stable. This behaviour is observed for a clean film/a contaminated film over both an impermeable and a porous substrate. It is to be noted that, in the presence of an insoluble surfactant, inertia delays the onset of instability for films over an impermeable as well as a porous substrate. The presence of the surfactant raises the critical Reynolds number for the occurrence of instability.

It is interesting to note that the critical Reynolds number where the instability first occurs for a contaminated film over a porous substrate is less than that for a contaminated film over an impermeable substrate. The above trend is noticed for all values of the Darcy numbers (δ)($\delta = 4 \times 10^{-3}, 10^{-2}$) considered. At a fixed Reynolds number, in the region where the Yih mode dominates, an increase in δ increases the growth rate; but the critical Reynolds number, at which the growth rate is zero decreases with an increase in δ. This indicates the destabilizing effect of the permeability of the porous substrate (δ) on a clean/a contaminated film at this value of $\hat{d}(\hat{d} = 0.05)$ and $\lambda = 0$ (Fig. 3(a)). Figure 3(b) presents the results for $\chi = 0.5$ and $\lambda = 0.5$ with the other parameters fixed as that in Fig. 3(a). For all the values of δ considered in the present study, the Reynolds number at which the growth rate is zero decreases with an increase in χ at this value of $\hat{d}(\hat{d} = 0.05)$. It is to be noted that this is not the trend which is observed for all the values of $\hat{d}$ considered, as is evident from Table I.

It is of interest to examine the effects of the thickness of the porous layer on the growth rate for a film over a porous substrate. Figure 4(a) ($\chi = 0.1$, $\lambda = 0$) and Figure 4(b) ($\chi = 0.5$, $\lambda = 0$) show the effects of $\hat{d}$ on the growth rate of the Yih and the Marangoni modes for a clean/a contaminated film over a porous substrate, when $\delta = 4 \times 10^{-3}$ for k $= 0.5$, $\alpha = 100$, Ca $= 2$, $\theta = 45^\circ$. Here, the solid curves (dashed curves) represent the results for a clean (a contaminated) film over a porous substrate. Y(Ma, $\hat{d}$) and M(Ma, $\hat{d}$) represent, respectively, the results for the Yih and the Marangoni modes at this value of $\hat{d}$ for a clean (Ma $= 0$) and a contaminated (Ma $= 1$) film over a porous substrate. The solid curves (for Ma $= 0$, $\hat{d} = 0.008$, $\hat{d} = 0.1$) in Figs. 4(a) and 4(b) represent the results of the growth rate of the Marangoni mode for a clean film over porous substrates with dimensionless thickness parameter $\hat{d} = 0.008$, $\hat{d} = 0.1$. As $\hat{d}$ increases, the growth rate for the Yih mode decreases in the region where the Yih mode dominates (where the growth rate is positive), indicating that there is a decrease in the growth rate with decrease in the thickness of the porous layer. Thus, the thicker the porous layer is, the more is the growth rate at any fixed Reynolds number where the Yih mode dominates. Further, as the thickness of the porous layer increases, the critical Reynolds number decreases. The above trend is exhibited by both clean and contaminated films over a porous substrate. Further, as observed earlier, for any thickness of the porous layer, the presence of the surfactant on the film over a porous layer delays the onset of instability. It is also noted that, an increase in χ (Fig. 4(b), $\chi = 0.5$) results in an increase in the growth rate of the Yih mode for a clean/a contaminated film over a thicker porous layer in the region where the Yih mode dominates.

Figure 5 presents the neutral stability curves for a clean (Fig. 5(a)) and a contaminated film (Fig. 5(b)) for a flow down a slippery substrate. It is observed that as β, the dimensionless slip

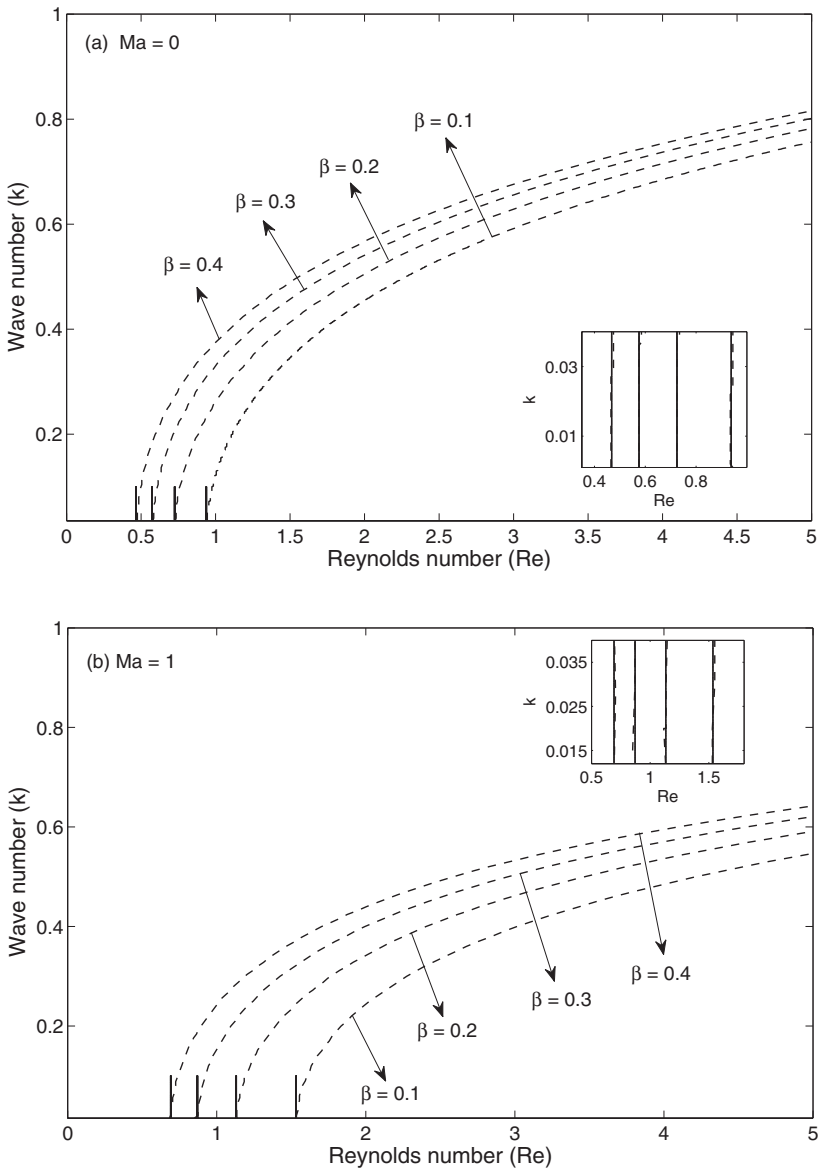

FIG. 5. Neutral stability curves for (a) a clean and (b) a contaminated film for flow over a slippery substrate when $\theta = 45^\circ$, Ca = 2. The solid curves represent the results of the long-wave analysis and dashed curves correspond to the solution of the Orr-Sommerfeld system.

coefficient increases, the critical Reynolds number decreases (dashed curves), indicating the destabilizing effect of β. The results of the long-wave analysis are incorporated in Fig. 5 (solid curves) and for small wave numbers, a good agreement between the two results is observed (see the inset).

The neutral stability maps are presented in Figs. 6 and 7 for a clean film (Ma = 0; Figs. 6(a)–6(c)) and for a contaminated film (Ma = 1; Figs. 7(a)–7(c)) over a porous substrate for different dimensionless thickness of the porous layer $\hat{d}$. They are presented in the cut-off wave number versus Reynolds number plane. The effects of the permeability are examined at each $\hat{d}$. The results for a clean and a contaminated film over an impermeable substrate are also incorporated (solid curve) in

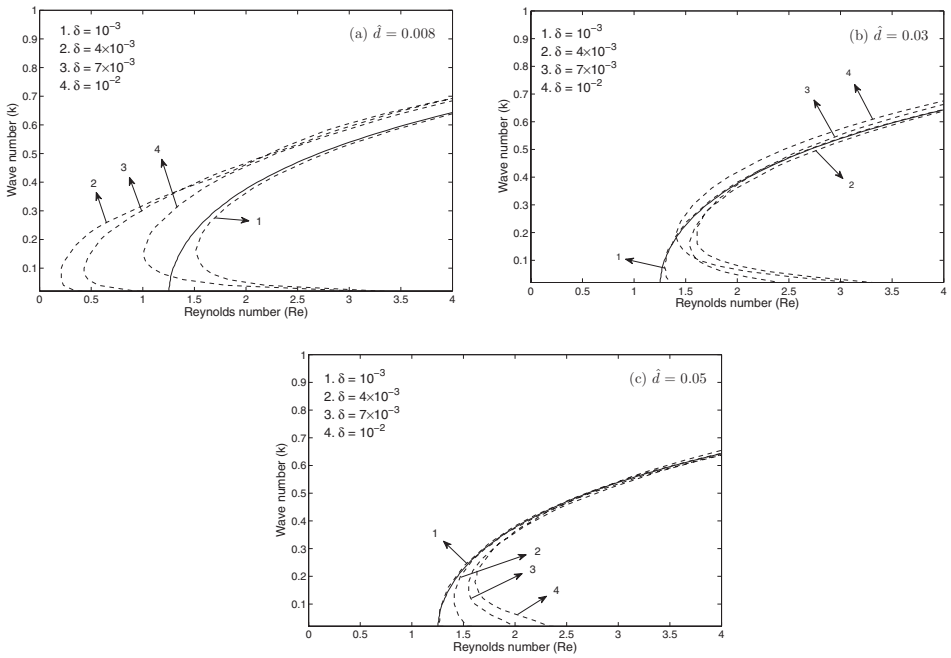

FIG. 6. Neutral stability curves when $\alpha = 1.0$, Ca $= 2$, $\theta = 45^{\circ}$, for a clean film over an impermeable substrate (solid curve; Blyth and Pozrikidis[9]) and over a porous substrate (dashed curves; $\lambda = 0.0$, $\chi = 0.1$). (a) $\hat{d} = 0.008$, (b) $\hat{d} = 0.03$, and (c) $\hat{d} = 0.05$.

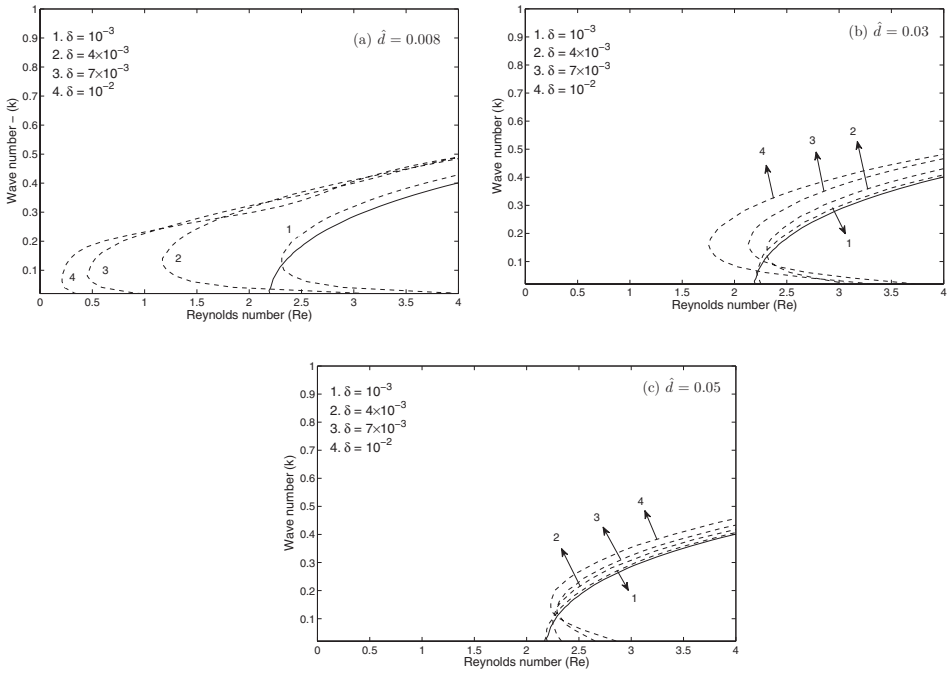

FIG. 7. Neutral stability curves when $\alpha = 1.0$, Ca $= 2$, $\theta = 45^{\circ}$, for a contaminated film over a rigid substrate (solid curve; Blyth and Pozrikidis[9]) and over a porous substrate (dashed curves; $\lambda = 0.0$, $\chi = 0.1$). (a) $\hat{d} = 0.008$, (b) $\hat{d} = 0.03$, and (c) $\hat{d} = 0.05$.

Figs. 6 and 7, respectively. The porous substrate characteristics are taken as $\lambda = 0$, $\chi = 0.1$, and the other parameters are $\alpha = 1$, Ca = 2, and $\theta = 45$. The results help one to find the range of unstable wave numbers for films over impermeable or porous substrates and also to find the critical Reynolds number above which the system is unstable. In each figure in Figs. 6 and 7, the region above or to the left of any curve is a stable region (where disturbances of wave number k decay with time) and the region below or to the right of any curve is an unstable region (where disturbances of wave number k are amplified with time) for the chosen parameter values. The point at which a curve meets the $k = 0$ axis gives the value of the critical Reynolds number.

The results are presented for $\hat{d} = 0.008$, $\hat{d} = 0.03$, and $\hat{d} = 0.05$ in Figs. 6(a)–6(c), respectively. When $\hat{d} = 0.008$ (Fig. 6(a)), the marginal stability curves are tugged towards the wave number axis for small wave numbers. It is observed that, the critical Reynolds number decreases with an increase in δ, showing the destabilizing effect of the presence of the porous substrate, for the flow of a clean film over it. Thus, at this value of $\hat{d}$, the effect of the permeability is to promote the instability close to its onset. However, the range of unstable wave numbers is reduced as δ increases from $\delta = 7 \times 10^{-3}$ to $\delta = 10^{-2}$ and is therefore stabilizing beyond certain values of the Reynolds numbers. Further, a clean film over a porous substrate is more unstable than a clean film over an impermeable substrate for larger values of the permeability parameter ($\delta = 10^{-2}$, $\delta = 7 \times 10^{-3}$ curves 3 and 4), at all the wave numbers considered. For $\delta = 10^{-3}$, a clean film over a porous substrate stabilizes the modes which were unstable for a clean film over an impermeable substrate. The region of unstable modes for $\delta = 10^{-3}$ is smaller than that for a clean film over an impermeable substrate. A clean film over an impermeable substrate is more unstable than that over a porous substrate ($\delta = 4 \times 10^{-3}$), for small wave numbers, whereas beyond this value of k, the region of unstable modes is larger for a clean film over a porous substrate than that over an impermeable substrate.

As $\hat{d}$ increases to $\hat{d} = 0.03$ (Fig. 6(b)), the critical Reynolds number exhibits a non-monotonic behaviour. As δ increases from $\delta = 10^{-3}$ to $\delta = 7 \times 10^{-3}$, the critical Reynolds number increases and therefore the presence of the porous substrate tends to stabilize but with further increase in δ to $\delta = 10^{-2}$, the critical Reynolds number decreases and this is destabilizing. This effect occurs at small wave numbers. Beyond a certain value of k, the range of unstable wave numbers is reduced for $\delta = 4 \times 10^{-3}$ than for $\delta = 10^{-3}$, and for a further increase in δ from $\delta = 4 \times 10^{3}$ to $\delta = 10^{-2}$, the range of unstable wave numbers increases and is thus destabilizing. Further, there is a window of stability for a clean film over a porous substrate for small values of wave numbers (in the sense that the critical Reynolds number for a clean film over a porous substrate is larger than that for a clean film over an impermeable substrate). In this window, the critical Reynolds number exhibits a non-monotonic behaviour. Outside this window of stability, a clean film over a porous substrate ($\delta = 7 \times 10^{-3}$ and $\delta = 10^{-2}$) is more unstable than that for a clean film over an impermeable substrate, and in this region, as δ increases, the region of unstable modes increases. With further increase in $\hat{d}$ to $\hat{d} = 0.05$ (Fig. 6(c)), the critical Reynolds number increases with increase in δ (from $\delta = 10^{-3}$ to $\delta = 10^{-2}$; exhibits monotonic behaviour) for small wave numbers. Thus, the effect of the Darcy number is to stabilize the film flow system for small wave numbers at this $\hat{d} = 0.05$. Beyond a certain value of k_c, at higher Reynolds numbers, as permeability increases, the range of unstable wave number decreases (for an increase of δ from $\delta = 10^{-3}$ to $\delta = 7 \times 10^{-3}$), but with a further increase to $\delta = 10^{-2}$, the range of unstable wave number increases.

The above results reveal that for a thick porous layer, an increase in permeability tends to destabilize the film flow system for a clean film. As the thickness of the porous layer reduces, permeability tends to stabilize the film flow system for large permeability values at small wave numbers but it is destabilizing at higher Reynolds numbers, although there is a non-monotonic behaviour. With further increase in $\hat{d}$, that is, for a thin porous layer, permeability tends to stabilize the film flow system at small wave numbers.

It is observed from Figs. 7(a)–7(c) that, when the film is contaminated, the critical Reynolds number increases (compared to the corresponding critical Reynolds number for Ma = 0) and the neutral curve is shifted to the right away from the wave number axis. This indicates the stabilizing role played by the surfactant. The results for the contaminated film are analogous (Figs. 7(a)–7(c)) to those for a clean film over a porous substrate for each $\hat{d}$ value considered in Figs. 6(a)–6(c) for small wave numbers. Beyond a certain value of k_c, an increase in the Darcy number tends to reduce the

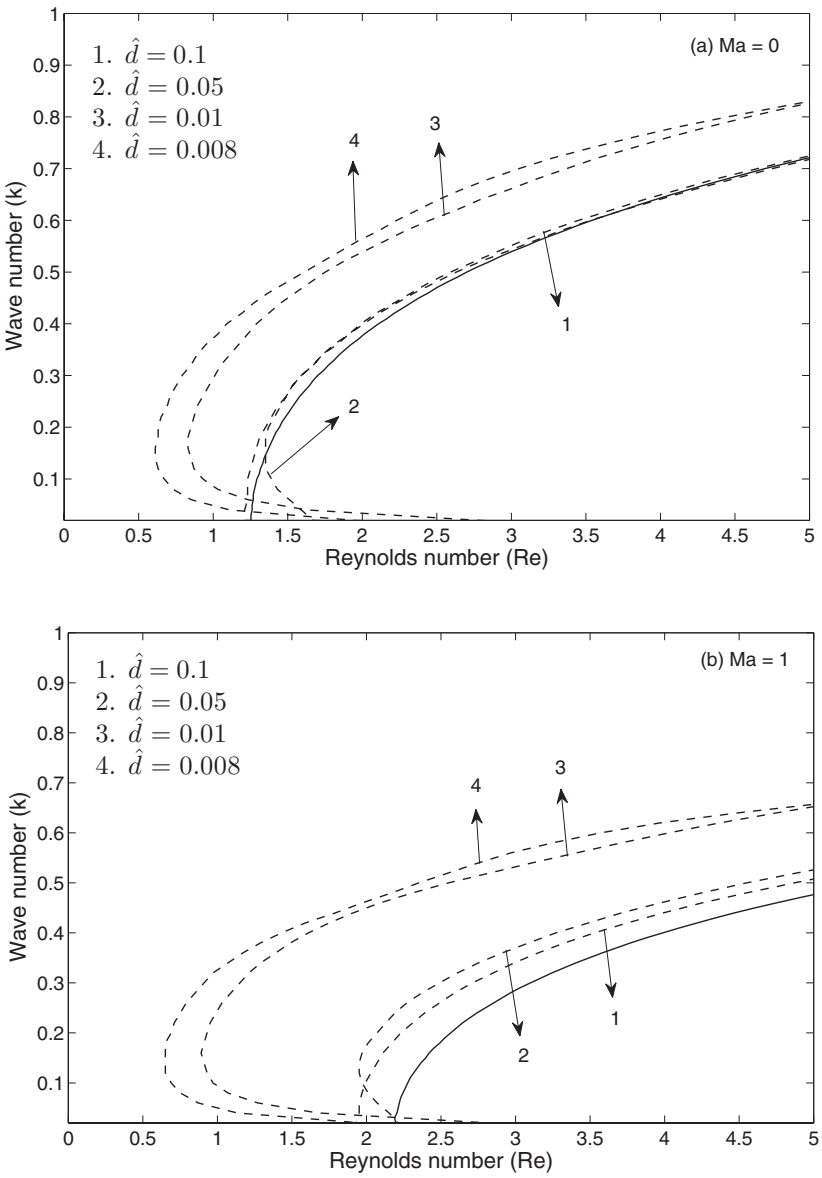

FIG. 8. Neutral stability curves when $\alpha = 1.0$, Ca $= 2$, $\theta = 45^{\circ}$, for (a) a clean and (b) a contaminated film over a porous substrate with $\delta = 7 \times 10^{-3}$, $\lambda = 0.0$, $\chi = 0.5$. The solid curve represents the results for a film over an impermeable substrate (Blyth and Pozrikidis[9]).

range of unstable wave numbers and exhibits a monotonic behaviour. Thus, a clean/a contaminated film over a thick porous layer is more unstable than over a thin porous layer for small wave numbers. Also, for a fixed porous layer thickness, a decrease in $\hat{d}$ corresponds to a decrease in the thickness of the fluid layer. Therefore, the above results can also be interpreted as follows, namely, a thin liquid film is more unstable than a thicker one over a porous substrate, of constant thickness, for small wave numbers.

The neutral stability curves in the cut-off wave number-Reynolds number window are presented for different values of $\hat{d}$ in Figs. 8(a) and 8(b) for Ma $= 0$ and Ma $= 1$, respectively, when

TABLE II. Values of critical Reynolds number as λ varies when $\hat{d} = 0.01$, $\chi = 0.1$, $\theta = 45^\circ$.

$\lambda \rightarrow$		0	0.25	0.5	0.75	0.9
$\delta = 10^{-3}$	Ma = 0	2.691	2.651	2.611	2.571	2.551
	Ma = 1	3.511	3.471	3.431	3.371	3.331
$\delta = 4 \times 10^{-3}$	Ma = 0	4.111	3.711	3.291	2.851	2.571
	Ma = 1	4.251	3.831	3.391	2.931	2.671
$\delta = 7 \times 10^{-3}$	Ma = 0	1.571	1.371	1.171	0.991	0.871
	Ma = 1	1.591	1.391	1.191	0.991	0.891

$\chi = 0.5, \lambda = 0, \mathrm{Ca} = 2, \alpha = 1$, and $\theta = 45^\circ$. The results show that the range of unstable wave numbers increases with a decrease in $\hat{d}$, indicating that as the porous layer thickness increases, the film flow system becomes more unstable at this value of $\delta = 7 \times 10^{-3}$ and $\chi = 0.5$. There is a k-Re window for small wave numbers, where a different scenario is observed, namely, the critical Reynolds number for $\hat{d} = 0.01$ is more than that for $\hat{d} = 0.008$ showing the stabilizing effect with increase in $\hat{d}$. But, with further increase to $\hat{d} = 0.05$, the critical Reynolds number decreases indicating the destabilizing effect in this k-Re window. Thus, in this k-Re window, a contaminated film over a thinner porous layer is more unstable. In the presence of the surfactant (Fig. 8(b)), the same trend as in Fig. 8(a) is observed but the contaminated film is more stable than a clean film at all $\hat{d}$ values considered. By comparing the results for $\chi = 0.1$ (Fig. 6(a)), $\chi = 0.5$ (Fig. 8(a)) when $\hat{d} = 0.008$ for $\delta = 7 \times 10^{-3}$ and Ma = 0, it is observed that the critical Reynolds number increases with an increase in χ indicating the stabilizing effect for small wave numbers; however, the range of unstable wave numbers increases with an increase in χ beyond a certain value of k_c. The same trend is observed for a contaminated film (Ma = 1; Figs. 7(a) and 8(b)). With further increase in χ, the trend is reversed (see Table I). The effects of the porosity (χ) and the stress-jump coefficient (λ) on the stability of the film flow system over an impermeable/a porous substrate are inferred from Tables I and II.

Table I shows the values of the critical Reynolds number for different values of χ (parameter describing the effects of porosity), as δ and $\hat{d}$ vary when k = 0.02. As χ increases, there is a decrease in the critical Reynolds number for $\hat{d} = 0.05$ and $\hat{d} = 0.1$ for the values of δ considered, indicating the destabilizing effect of the porosity on the film over a thin porous layer. But for $\hat{d} = 0.01$, as χ increases, from 0.1 to 0.2, the critical Reynolds number for a clean film over a porous substrate increases for the values of δ considered and then with further increase in χ to $\chi = 0.5$, the critical Reynolds number decreases. For this value of $\hat{d}$, when Ma = 1, this trend is observed only for $\delta = 4 \times 10^{-3}$, whereas, for the other δ values, as χ increases, the critical Reynolds number increases. This shows that, as the porosity of the porous substrate increases, the film flow system is in general destabilized both for a clean and a contaminated film but at smaller permeability values, there is a non-monotonic behaviour exhibited by the critical Reynolds number. The results, thus reveal that by appropriate choice of the values of the porosity and the permeability parameters, it is possible to obtain a k-Re window in which both a clean and a contaminated film over a porous substrate can be stabilized and outside this window of stability, there is a possibility of enhancing the destabilizing effect of the film flow system. The region of k-Re window where the film is stabilized can be enlarged or decreased by properly choosing the thickness of the porous substrate.

The stress-jump coefficient λ is another parameter that plays a vital role in the stability of the film flow system. Table II shows the critical Reynolds number values as λ varies, for different values of δ, when $\hat{d} = 0.01$. The results show that, with an increase in λ, the critical Reynolds number decreases, indicating the destabilizing effect of λ on a clean/a contaminated film over a thick porous layer.

IV. CONCLUSIONS

The linear stability of a clean/a contaminated liquid film flowing down an inclined porous substrate is examined and the Chebyshev-Tau spectral method is employed to obtain the results for

the growth rate of the disturbances and the critical Reynolds number values for different values of the parameters characterizing the porous medium. The growth rate of the Marangoni mode is always negative and remains a constant for fixed values of δ, $\hat{d}$, and χ. The Yih mode is dominated by the Marangoni mode for small Reynolds numbers. As Reynolds number increases, the growth rate of the Yih mode increases, it overtakes the Marangoni mode, and from then on, the growth rate of the Yih mode is positive and it becomes the dominant mode. This happens for both a clean and a contaminated film over a porous/an impermeable substrate. It is observed that the presence of the surfactant tends to stabilize the film flow over a porous substrate. The influence of the other parameters characterizing the porous substrate such as the Darcy number δ, the porosity χ, the ratio of the liquid layer to the porous layer thickness $\hat{d}$ and the stress-jump coefficient λ, show that by properly choosing the above parameter values, it is possible to find a k-Re window for small wave numbers, where a clean/a contaminated film over a porous substrate can be stabilized in comparison to that of a clean/a contaminated film over an impermeable substrate. Outside this window, the destabilizing influence of the presence of the porous substrate on a clean/a contaminated film can be enhanced. In view of the above, one can consider a clean/a contaminated film over a porous substrate with appropriate values for the porous medium characteristics and use it as a strategy for stabilizing/destabilizing the film flow system above it, in accordance with the application for which this configuration is useful and relevant.

ACKNOWLEDGMENTS

The authors sincerely thank the referees for their valuable suggestions and useful comments. These have helped in improving the quality and presentation of the results in the manuscript. The authors also thank the editor for his useful suggestions and encouraging remarks.

APPENDIX A: PLANE-PARALLEL FLOW OF A FILM OVER A POROUS SUBSTRATE

The equations and the boundary conditions corresponding to the plane-parallel flow of a film with uniform thickness over a porous substrate are obtained from Eqs. (18)–(33) and are given by

$$u_{zz} + \mathrm{GRe} = 0, \tag{A1}$$

$$p_z + \mathrm{GRe}\cot\theta = 0, \tag{A2}$$

$$u_z = 0, \ \text{on } z = 1, \tag{A3}$$

$$p = 0, \ \text{on } z = 1, \tag{A4}$$

$$U_{z_b z_b} - \frac{\chi}{\delta^2} U = -\frac{\mathrm{GRe}^2}{\hat{d}^3}\chi, \tag{A5}$$

$$P_{z_b} + \frac{\mathrm{GRe}^2}{\hat{d}^3}\cot\theta = 0, \tag{A6}$$

$$u_z = \frac{\hat{d}}{\mathrm{Re}} U, \ \text{on } z = z_b = 0, \tag{A7}$$

$$U_{z_b} - \frac{\mathrm{Re}\chi}{\hat{d}^2} u_z = \frac{\lambda\chi}{\delta} U, \ \text{on } z = z_b = 0, \tag{A8}$$

$$p = \frac{\hat{d}^2}{\mathrm{Re}^2} P, \ \text{on } z = z_b = 0, \tag{A9}$$

$$\Gamma = 1, \ \text{on } z = 1, \tag{A10}$$

$$U = 0, \ \text{on } z_b = -1. \tag{A11}$$

The solutions u_B of (A1) and U_B of (A5) subject to the conditions (A3), (A7), (A8), and (A11) are obtained and are given by Eqs. (34) and (35).

APPENDIX B: O(1) AND O(k) PROBLEMS

Substituting Eq. (76) in the Orr-Sommerfeld system of Eqs. (64)–(75), the equations at O(1) and at O(k) are obtained. The equations at O(1) are given by

$$\phi_0'''' = 0, \tag{B1}$$

$$\phi_0(1) + \zeta_0\Big[u_B(1) - c_0\Big] = 0, \text{ on } z = 1, \tag{B2}$$

$$\phi_0'''(1) = 0, \text{ on } z = 1, \tag{B3}$$

$$u_B''(1)\zeta_0 + \phi_0''(1) = 0, \text{ on } z = 1, \tag{B4}$$

$$\phi_0'(1) + \Gamma_0\Big[u_B(1) - c_0\Big] = 0, \text{ on } z = 1, \tag{B5}$$

$$\phi_0^{b\,''''} - \frac{\chi}{\delta^2}\phi_0^{b\,''} = 0, \tag{B6}$$

$$\phi_0{}''' = \frac{\hat{d}^3}{\mathrm{Re}\chi}\phi_0^{b\,'''} - \frac{\hat{d}^3}{\mathrm{Re}\delta^2}\phi_0^{b\,'}, \text{ on } z = z_b = 0, \tag{B7}$$

$$\mathrm{Re}\phi_0 = \phi_0^b, \text{ on } z = z_b = 0, \tag{B8}$$

$$\mathrm{Re}\phi_0{}' = \hat{d}\phi_0^{b\,'}, \text{ on } z = z_b = 0, \tag{B9}$$

$$\phi_0{}'' - \frac{\hat{d}^2}{\mathrm{Re}\chi}\phi_0^{b\,''} = -\frac{\lambda}{\delta}\frac{\hat{d}^2}{\mathrm{Re}}\phi_0^{b\,'}, \text{ on } z = z_b = 0, \tag{B10}$$

$$\phi_0^b = 0, \text{ on } z_b = -1, \tag{B11}$$

$$\phi_0^{b\,'} = 0, \text{ on } z_b = -1. \tag{B12}$$

The equations at O(k) are given by

$$\phi_1'''' = i\mathrm{Re}\Big[u_B - c_0\Big]\phi_0{}'' - i\mathrm{Re}u_B''\phi_0, \tag{B13}$$

$$\phi_1(1) = c_1\zeta_0 - \Big[u_B(1) - c_0\Big]\zeta_1, \text{ on } z = 1, \tag{B14}$$

$$\phi_1''' = i\mathrm{Re}\Big[u_B(1) - c_0\Big]\phi_0{}'(1) + 2i\cot\theta\zeta_0, \text{ on } z = 1, \tag{B15}$$

$$\phi_1''(1) + u_B''(1)\zeta_1 + \frac{i\mathrm{Ma}}{\mathrm{Ca}}\Gamma_0 = 0, \text{ on } z = 1, \tag{B16}$$

$$\phi_1'(1) - \Gamma_0(c_1 + \frac{i}{\alpha\mathrm{Ca}}) + \Gamma_1\Big[u_B(1) - c_0\Big] = 0, \text{ on } z = 1, \tag{B17}$$

$$\phi_1^{b\,''''} - \frac{\chi}{\delta^2}\phi_1^{b\,''} + \frac{ic_0\mathrm{Re}}{\hat{d}^2}\phi_0^{b\,''} = 0, \tag{B18}$$

$$\phi_1{}''' + \mathrm{Re}u_B'(0)i\phi_0 - i\mathrm{Re}\Big[u_B(0) - c_0\Big]\phi_0' = \frac{\hat{d}^3}{\mathrm{Re}}\Big[\frac{1}{\chi}\phi_1^{b\,''''} - \frac{1}{\delta^2}\phi_1^{b\,'} + \frac{ic_0\mathrm{Re}}{\hat{d}^2\chi}\phi_0^{b\,'}\Big], \text{ on } z = z_b = 0, \tag{B19}$$

$$\mathrm{Re}\phi_1 = \phi_1^b, \text{ on } z = z_b = 0, \tag{B20}$$

$$\mathrm{Re}\phi_1{}' = \hat{d}\phi_1^{b'}, \text{ on } z = z_b = 0, \tag{B21}$$

$$\phi_1{}'' - \frac{\hat{d}^2}{\mathrm{Re}\chi}\phi_1^{b''} = -\frac{\lambda}{\delta}\frac{\hat{d}^2}{\mathrm{Re}}\phi_1^{b'}, \text{ on } z = z_b = 0, \tag{B22}$$

$$\phi_1^{b'} = 0, \text{ on } z_b = -1, \tag{B23}$$

$$\phi_1^b = 0, \text{ on } z_b = -1. \tag{B24}$$

The solutions to (B13) and (B18) are given by Eqs. (84) and (85) and the constants appearing in (84) and (85) are given by

$$\begin{aligned}
a_1 &= -i\mathrm{Re}\Gamma_0\Big[u_B(1) - c_0\Big]\Big[1 - (c_0 - u_B(1))\Big] + 2i\zeta_0\cot\theta,\\
a_2 &= i\mathrm{Re}\Gamma_0\Big[u_B(1) - c_0\Big]\Big[\frac{1}{3} - (c_0 - u_B(1))\Big] + 2\zeta_1 - \frac{i\mathrm{Ma}}{\mathrm{Ca}}\Gamma_0 - 2i\zeta_0\cot\theta,\\
a_3 &= \frac{\hat{d}}{\mathrm{Re}}\Big[\sqrt{p}(b_1 - b_2) + b_3 + \frac{ic_0\mathrm{Re}^2\delta^3}{2\hat{d}^4\sqrt{\chi}}\frac{u_B''(1)(E_+ - E_-)\zeta_0}{\Delta}\Big],\\
a_4 &= \frac{1}{\mathrm{Re}\Delta}\Big[A\{-\lambda\sqrt{\chi}(E_+ + E_- - 2) + (E_+ - E_-)\}\Big]\\
&\quad + \frac{K}{\Delta\mathrm{Re}}(E_+ + E_- - 2) - \frac{2i\cot\theta\zeta_0\delta^2}{\hat{d}^3},\\
b_1 &= \frac{AB_+ + KE_+}{\Delta}, \quad b_2 = \frac{KE_- - AB_-}{\Delta},\\
b_3 &= -\frac{2i\cot\theta\zeta_0 Re\delta^2}{\hat{d}^3}, \quad b_4 = \mathrm{Re}a_4 - b_1 - b_2,\\
A &= -\frac{2ic_0\mathrm{Re}^2\delta^3\zeta_0}{\hat{d}^4\sqrt{\chi}\Delta} + \frac{2i\cot\theta\zeta_0\mathrm{Re}\delta^3}{\hat{d}^3\sqrt{\chi}},\\
K &= \frac{\delta^2\mathrm{Re}}{\hat{d}^2}\Big[a_2 + \frac{\lambda\hat{d}^2}{\delta\mathrm{Re}}b_3 - \frac{ic_0\mathrm{Re}\delta^2u_B''(1)\zeta_0}{\hat{d}^2\chi\Delta}\{(E_+ + E_-) - \frac{\lambda\sqrt{\chi}}{2}(E_+ - E_-)\}\Big].
\end{aligned} \tag{B25}$$

[1] S. V. Alekseenko, V. E. Nakoryakov, and B. G. Pokusaev, *Wave Flow in Liquid Films*, 3rd ed. (Begell House, New York, 1994).
[2] A. Oron, S. H. Davis, and S. G. Bankoff, "Long scale evolution of thin films," Rev. Mod. Phys. **69**, 931 (1997).
[3] H. C. Chang and E. A. Demekhin, *Complex Wave Dynamics on Thin Films*, 1st ed. (Elsevier, Amsterdam, The Netherlands, 2002).
[4] R. V. Craster and O. K. Matar, "Dynamics and stability of thin liquid films," Rev. Mod. Phys. **81**, 1131 (2009).
[5] P. Gao and Xi. Y. Li, "Effect of surfactants on the long-wave stability of oscillatory film flow," J. Fluid Mech. **562**, 345 (2006).
[6] E. A. Demekhin, S. Kalliadasis, and M. G. Velarde, "Suppressing falling film instabilities by Marangoni forces," Phys. Fluids. **18**, 042111 (2006).
[7] V. Shankar and A. K. Sahu, "Suppression of instability in liquid flow down an inclined plane by a deformable solid layer," Phys. Rev. E **73**, 016301 (2006).
[8] Gaurav and V. Shankar, "Role of wall deformability on interfacial instabilities in gravity-driven two-layer flow with a free surface," Phys. Fluids **22**, 094103 (2010).
[9] M. G. Blyth and C. Pozrikidis, "Effect of surfactant on the stability of film flow down an inclined plane," J. Fluid Mech. **521**, 241 (2004).
[10] H. H. Wei, "Effect of surfactant on the long-wave instability of a shear-imposed liquid flow down an inclined plane," Phys. Fluids **17**, 012103 (2005).
[11] S. H. Davis, "Thermocapillary instabilities," Annu. Rev. Fluid. Mech. **19**, 403 (1987).

[12] T. B. Benjamin, "Effect of surface contamination on wave formation in falling liquid films," Archwm. Mech. Stosow. **16**, 615 (1964).
[13] S. Whitaker, "Effect of surface-active agents on the stability of falling liquid films," Ind. Eng. Chem. Fundam. **3**, 132 (1964).
[14] S. Whitaker and L. O. Jones, "Stability of falling liquid films. Effect of interface and interfacial mass transport," AIChE J. **12**, 421 (1966).
[15] S. P. Lin, "Stabilizing effects of surface-active agents on a film flow," AIChE J. **16**, 375 (1970).
[16] C. Pozrikidis, "Effect of surfactants on film flow down a periodic wall," J. Fluid Mech. **496**, 105 (2003).
[17] W. Ji and F. Setterwall, "On the instabilities of vertical falling liquid films in the presence of surface-active solute," J. Fluid Mech. **278**, 297 (1994).
[18] A. L. Frenkel and D. Halpern, "Stokes flow instability due to interfacial surfactant," Phys. Fluids **14**, L45 (2002).
[19] D. Halpern and A. L. Frenkel, "Effect of inertia on the insoluble surfactant instability of shear flow," Phys. Rev. E **71**, 016302 (2005).
[20] D. Halpern and A. L. Frenkel, "Destabilization of a creeping flow by interfacial surfactant: linear theory extended to all wavenumbers," J. Fluid Mech. **485**, 191 (2003).
[21] M. G. Blyth and C. Pozrikidis, "Effect of surfactants on the stability of the two-layer channel flow," J. Fluid Mech. **505**, 59 (2004).
[22] C. Pozrikidis, "Effect of inertia on the Marangoni instability of the two-layer channel flow. Part I. Numerical simulations," J. Eng. Math. **50**, 311 (2004).
[23] M. G. Blyth and C. Pozrikidis, "Effect of inertia on the Marangoni instability of the two-layer channel flow. Part II. Normal-mode analysis," J. Eng. Math. **50**, 329 (2004).
[24] J. P. Pascal, "Linear stability of fluid flow down a porous inclined plane," J. Phys. D: Appl. Phys. **D32**, 417 (1999).
[25] J. P. Pascal, "Instability of power-law fluid flow down a porous incline," J. Non-Newtonian Fluid Mech. **133**, 109 (2006).
[26] I. M. R. Sadiq and R. Usha, "Thin Newtonian film flow down a porous inclined plane: stability analysis," Phys. Fluids **20**, 022105 (2008).
[27] I. M. R. Sadiq, R. Usha, and S. W. Joo, "Instabilities in a liquid film flow over an inclined heated porous substrate," Chem. Eng. Sci. **65**, 4443 (2010).
[28] J. P. Pascal and S. J. D. D'Alessio, "Instability in gravity-driven flow over uneven permeable surfaces," Int. J. Multiphase Flow **36**, 449 (2010).
[29] A. Samanta, C. R. Quil, and B. Goyeau, "A falling film down a slippery inclined plane," J. Fluid Mech. **684**, 353 (2011).
[30] R. Liu and Q. Liu, "Instabilities of liquid film flowing down an inclined porous plane," Phys. Rev. E **80**, 036316 (2009).
[31] G. S. Beavers and D. D. Joseph, "Boundary conditions at a naturally permeable wall," J. Fluid. Mech. **30**, 197–207 (1967).
[32] S. Whitaker, *The Method of Volume Averaging* (Kluwer Academic, Dordrecht, The Netherlands, 1999).
[33] B. Goyeau, D. Lhuillier, D. Gobin, and M. G. Velarde, "Momentum transport at a fluid-porous interface," Int. J. Heat Mass Transfer **46**, 4071 (2003).
[34] J. A. Ochoa-Tapia and S. Whitaker, "Momentum transfer at the boundary between a porous medium and a homogeneous fluid-I. Theoretical development," Int. J. Heat Mass Transfer **38**, 2635 (1995).
[35] F. J. Valdés-Parada, B. Goyeau, and J. A. Ochoa-Tapia, "Jump momentum boundary condition at a fluid-porous dividing-surface: derivation of the closure problem," Chem. Eng. Sci. **62**, 4025 (2007).
[36] F. J. Valdés-Parada, J. Alvarez-Ramirez, B. Goyeau, and J. A. Ochoa-Tapia, "Computation of jump coefficients for momentum transfer between a porous medium and a fluid using a closed generalized transfer equation," Transp. Porous Media **78**, 439 (2009).
[37] U. Thiele, B. Goyeau, and M. G. Velarde, "Stability analysis of thin film flow along a heated porous wall," Phys. Fluids **21**, 014103 (2009).
[38] S. Whitaker, "The Forchheimer equation: A theoretical derivation of Darcy' s law," Transp. Porous Media **25**, 27 (1996).
[39] P. Bousquet-Melou, B. Goyeau, M. Quintard, F. Fichot, and D. Gobin, "Average momentum equation for interdendritic flow in a solidifying columnar mushy zone," Int. J. Heat Mass Transfer **45**, 3651 (2002).
[40] D. J. Benney, "Long waves on liquid films," J. Math. Phys. **45**, 150 (1966).
[41] A. W. Adamson, *Physical Chemistry of Surfaces* (Wiley-Interscience, New York, USA, 1990).
[42] D. A. Nield and A. Bejan, *Convection in Porous Media* (Springer-Verlag, New York, 1999).
[43] H. A. Stone, "A simple derivation of the time-dependent convective-diffusion equation for surfactanat transport along a deforming interface," Phys. Fluids **2**, 111 (1990).
[44] C. S. Yih, "Stability of liquid flow down an inclined plane," Phys. Fluids **6**, 321 (1963).
[45] P. J. Olsson and D. S. Henningson, "Optimal disturbance growth in watertable flow," Stud. Appl. Math. **94**, 183 (1995).
[46] T. B. Benjamin, "Wave formation in laminar flow down an inclined plane," J. Fluid Mech. **2**, 554 (1964).
[47] J. Liu, J. D. Paul, and J. P. Gollub, "Measurements of the primary instabilities of film flows," J. Fluid Mech. **250**, 69 (1993).
[48] R. W. Chin, F. H. Abernathy, and J. R. Bertschy, "Gravity and shear wave stability of free surface flows. Part 1. Numerical calculations," J. Fluid Mech. **168**, 501 (1986).